1984

Solar Zeolite Refrigeration System

J. A. Roux

Open-File Report 84-1S

Solar Zeolite Refrigeration System

J. A. Roux and S. C. Chang

1984

The Mississippi Mineral Resources Institute
University, Mississippi 38677

SOLAR ZEOLITE REFRIGERATION SYSTEM

by

J. A. Roux and S.C. Chang

University of Mississippi
University, MS

Mississippi Mineral Resources Institute
University of Mississippi
University, MS 38677

July, 1984

ABSTRACT

A solar powered zeolite-water absorption unit was designed to produce either a cooling or heating effect. The thermodynamic expressions related to cooling have been derived to predict the system performance. The operating range and optimum design parameters for the zeolite system were determined through both theoretical analysis and computer simulation. The main parameters governing performance were: solar collector type, ambient temperature , and absorber properties. The zeolite heat absorption value was determined from the slope of the constant mass line on a graph of log Pv versus 1/Ta. The system performance showed a weak dependence on the heat of absorption when using a single glazing flat-plate solar collector. The LiBr-water continuous cycle was found to have slightly better performance than the zeolite-water system but was also much more mechanically complex and may stop functioning during certain climate conditions. The zeolite intermittent cycle has slightly lower system performance than the LiBr-water system but has a wider operating range of generator and absorber temperatures and can be used to simultaneously produce domestic hot water and refrigeration.

TABLE OF CONTENTS

page

Abstract iv

List of Tables vii

List of Figures viii

Nomemclature x

Chapter

I. INTRODUCTION..... 1

II. STATEMENT OF THE PROBLEM..... 19

III. THERMODYNAMIC ANALYSIS..... 25

3.1 System Performance Based on Carnot Cycle.....25

3.2 The Absorption Refrigeration Cycle..... 26

3.3 Absorber Properties Equation..... ..40

3.4 Relationship Between Absorber and Absórbate Temperature..... 42

3.5 Relationship Between Solar Collector Efficiency and Absorption Properties.....51

3.6 Instantantous CP for Solar Zeolite Refrigeration System.....52

page

3.7 Mean CP for Solar Zeolite Refrigeration System.....53

IV. RESULTS AND DISCUSSION.....55

4.1 Comparison Between Two Methods of Determining Refrigerant Desorption Temperature.....55

4.2 Effect of Absorber Slope on the Refrigerant Desorption Temperature..... 57

4.3 Relationship Between System CP and Generator Temperature.....58

4.4 The Optimum Uniform Slope.....61

4.5 Effect of Non-Uniform Zeolite Slope..... 62

4.6 Effect of Ambient Temperature..... 67

4.7 Comparison Between the Zeolite(13X)-Water Intermittent and LiBr-Water Continuous Cycle.... 73

4.8 SystemSizing and Cost.....'..78

V. CONCLUSION 84

REFERENCES 88

VITA 91

LIST OF TABLES

Table page

I Classfication of Power Cycle in Various Solar Refrigeration Systems..... 5

II Cooling Load for a Typical 2000 ft. House..... 79

III Zeolite Mass Corresponding to the Cooling Load of Table II 79

IV P-Type Solar Refrigeration Collector Area..... 81

V S-Type Solar Refrigeration Collector Area..... 82

VI V-Type Solar Refrigeration Collector Area..... 83

LIST OF FIGURES

Figure page

1 Flow Chart for a Vapor-Compression Refrigeration Cycle Using Solar Energy..... 3

2 Effect of Sorbate Concentration on COP Intermittent Type.....10

3 Effect of Sorbate Concentration on COP Continuous Type..... 11

4 Typical Isotherms for Absorbed Mass Versus Vapor Pressure..... 13

5 Comparison of System COP for Three Absorption Refrigerators Without Using Solar Energy..... 15

6 The Solar Zeolite Absorption Refrigeration System..... 21

7 T-s Diagram for System Overall Performance, CPc as a function of Tg..... 27

8 Relationship Between Absorption Properties and Absorption Refrigeration Cycle.....29

9 Comparison for Two Carnot Refrigeration Cycles: (1) Power Cycle ($T_L = T$) (2)Power Cycle ($T_L = T_{ai}$)..... 31

10 T-s Diagram for Maximum Work of the Power Cycle in Absorption Refrigeration System.....36

11 Comparison Between Carnot Cycle and Absorption Cycle. 39

Figure page

12 The Log Pv Versus 1/Tz Plot for Zeolite
NaX-Water Pair..... ,....41
13 The Linear Relation Between Tv and Tab in the
Absorption Properties Equation..... 46
14 Tv Versus Tz for Zeolite 13X-Water Pair.....50
15 Comparison Between Eq.(31) (L dependent on T)
and Eq. (23) (Constant L).....:..... 56
16 Effect of the Slope, m, on Desorption
Temperature.....59
17 System CP Versus Generator Temperature..... 60
18 Idealizied Slope, mz Versus Peak CPm.....63
19 Effect of Non-Uniform Zeolite Slope..... 65
20 Ideal Slope as a Function of Ambient Temperature.... 68
21 Effect of Ambient Temperature (P-type Collector).... 70
22 Effect of Ambient Temperature (S-type Collector)....71
23 Effect of Ambient Temperature (V-type Collector).... 72
24 Comparison Between Zeolite-Water Intermittent ,
and LiBr-Water Continuous Cycles (P-Type)..... 74
25 Comparison Between Zeolite-Water Intermittent
and LiBr-Water Continuous Cycles (P,S,and V-Type)...76

Nomemclature

a = End point of absorption process in absorption cycle

b = Starting point of desorption process in absorption cycle

c = End point of desorption process in absorption cycle

C = Constant

Cco = Constant for the collector efficiency equation

C_L = Constant for the heat of vaporation equation (kj/kg) .

Cpz = Specific heat of zeolite (kj/kg 'K)

Cz = Constant for the zeolite-water property equation

CP = Instantaneous ratio of cooling effect to incident solar flux.

CPc = CP based on Carnot cycle limited by the ambient and heat source temperatures.

CPca = CP based on Carnot cycle according to absorption refrigeration cycle temperatures.

CPa = CP based on absorption refrigeration cycle.

CPm+ = Mean CP defined in Eq.3 8.

CPm = Mean CP defined in Eq.39.

COP = Ratio of cooling effect to heat comsumption of generator.

COPr = Ratio of cooling effect to work input.

COPc = System COP based on Carnot cycle.

COPa = System COP based on absorption refrigeration cycle.

d = Starting point of absorption process

in absorption cycle

e = Ln P / Log P

h = Enthalpy of water vapor (kj/kg)

ΔH = Heat of absorption (kj/kg)

L = Latent Heat of Vaporization (kj/kg)

m_{co} = Slope of a solar collector efficiency line

as a function of zeolite Temperature (°C)

m_L = Slope of heat of evaporarion line as a

function of water vapor Temperature (°C)

m_B = Slope of a constant mass line

on log P versus 1/Tplot(°K)

M = Mass (kg)

P = Pressure (bar)

Q = Heat (kj)

R = Water vapor gas constant (kj/kg,*K)

S = Entropy (kj/kg)

T = Temperature

T_H = High working temperature in Carnot cycle (*K)

T_L = Low working temperature in Carnot cycle (*K)

Ta = Absorption temperature ('K)

Tg = Desorption temperature at generator ('K)

Tza = Temperature at which absorption process ends ('K)

Tzb = Temperature at beginning of desorption (*K)

Tzc = Temperature at which desorption process ends (*K)

Tzd = Temperature at beginning of absorption (°K)

Xa = Weight ratio of ammonia to ammonia-water solution

Xz = Weight ratio of absorbed water to solid zeolite

Subscript

a = absorption

ab = absorber

c = condenser

C = Carnot

co = collector

e = evaporator

f = Liquid state, final state

g = Generator, gas

i = counter index

P = Power cycle

v = Vapor

w = Water

z = Zeolite

Greek symbols

? = Efficiency

PO = Ambient

CHAPTER I

INTRODUCTION

Energy prices have increased sharply since the 1973 energy crisis. Conservation practices have helped to reduce the rate of increase for the demand of energy. However, conservation is not a net producer of energy and it alone will not solve the energy problem in the long run. In a recent evaluation of the energy situation, the Office of Technology Assessment stated, "A transition between energy sources must occur during the next two or three decades because of the physical limit of supplies of low cost oil and natural gas" (1).

Two possible long-term solutions to the energy problem are solar-energy and nuclear-fusion. Nowadays nuclear-fusion still has many technological obstacles to overcome and solar-energy devices are not always economically realistic. The main difficulty for obtaining more economic benefit from solar energy is that solar energy is usually associated with relatively low temperatures and the system cost is not always economically competitive with presently available energy sources.

However, unlike applying solar energy to create electric power which requires high temperatures and expensive equipment, applying solar-energy techniques for refrigeration only requires relatively low temperatures and has four major advantages. (1) Solar energy can help to solve the peak electric power load problem during the summer season. (2) The available solar energy- and the required cooling are in phase. (3) Solar energy can reduce energy consumption in refrigeration and help to solve the long term energy problem by providing an alternative energy source. (4) In a highly agricultural country where electric power is undeveloped, adequate solar refrigeration facilities can avoid the waste of perishable food stuffs.

Many thermodynamic cycles are available for producing refrigeration. The vapor-compression refrigeration cycle requires the least amount of refrigerant (thus least size) and also has a good system performance. Since a net amount of work must be input into the vapor-compression refrigeration cycle,the solar energy input for this cycle must be converted into some form of work. Therefore a power cycle and a solar collector must be used in all solar vapor-compression refrigeration systems (including solar-absorption refrigeration) as illustrated in Fig 1 .

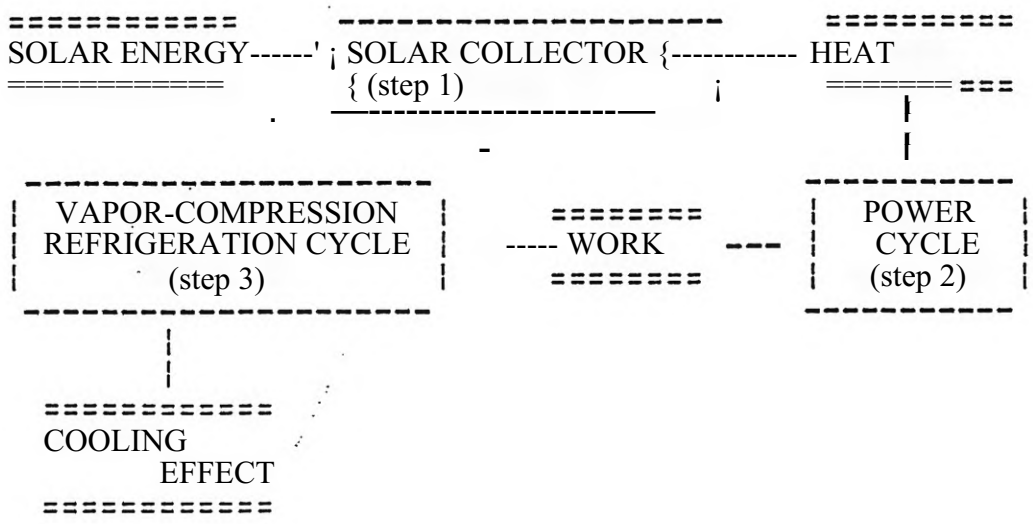

Fig 1. Flow Chart for a Vapor-Compression

Refrigeration Cycle Using Solar Energy

It is obvious from Fig. 1 that 3 steps of energy conversion are necessary to produce cooling from solar energy. The overall system performance (system CP) will equal the product of the 3 energy conversion factors, i.e.: (1) the efficiency of the solar collector (step 1), (2) the efficiency of the power cycle (step 2), and (3) the COP of the vapor-compression refrigeration cycle (step 3). To compare the system overall CP for different solar refrigeration systems, the first and last step energy conversion factors can be ignored because of only small mechanism variations in these two steps for different solar refrigeration concepts. For example, due to the economy and simplicity, the flat-plate solar collector mechanism has been used at step 1 for most solar refrigeration systems. At step 3 the cycle and mechanisms in different solar refrigeration systems are nearly the same except for the working fluid.

The mechanisms of compression may be different, but they can be assumed to belong to the operation at step 2. Since the theoretical COP of various refrigerents (the working fluid at step 3) are only slightly different in most solar refrigeration systems, the most significant variation for comparison of the different solar refrigeration systems is the energy conversion factor at step 2. Theoretically,

the power cycle at step 2 will have nearly the same working temperature range when using a flat-plate solar collector and hence nearly the same Carnot power cycle efficiency. However different solar refrigeration systems have different power cycle mechanisms and hence the losses in the actual power cycles are significantly different. Therefore the overall system CP for different solar refrigeration concepts depends strongly on the actual losses of their power cycles. Power cycle mechanisms can be classified into the mechanical and non-mechanical types as shown in Table I.

Table I . Classfication of Power Cycle in Various Solar Refrigeration Systems

Solar Refrigeration Systems	Power Cycle Type
1. Rankine powered solar refrigeration system	mechanical
2. Stirling solar refrigeration system	mechanical
3. Jet refrigeration system	non-mechanical
4. Solar desiccant refrigeration system	non-mechanical
5. Solar absorption refrigeration system	non-mechanical

In the power.cycle, mechanical systems have friction and pressure losses,' such as in the Stirling (Ref.2) .powered solar refrigeration system. These friction losses limit mechanical systems to use at high pressures (thus high temperatures) which cannot be easily achieved by solar collectors. High pressure losses can occur in the turbine of a Rankine powered solar refrigeration system, these pressure losses will increase sharply for a small size unit. The inefficiency and high cost for a small size turbine also limit these mechanical systems to use for large capacity refrigeration applications. Prigmore and Barber (3) have pointed out that the Rankine cycle powered refrigeration system will become more economical when thermal capacities are 100 tons or greater.

Conversely, a non-mechanical device in the power cycle can reduce mechanical friction and pressure losses but ,may suffer from fluid friction and irreversible heat transfer losses. This occurs in the jet refrigeration system, Ref. 4. The mixing (air and steam) losses and fluid friction losses in the nozzle also limit the jet system use to high pressure, high temperature steam which is not easy to obtain with a flat-plate solar collector. The desiccant cooling system, Refs. (5,6,7), is an open cycle absorption system. The working fluid in this open cycle absorption system is

air which only inçludes a small amount of refrigerant (water). Due to the large mass flow rates passing through the absorber bed in this open system, the fluid friction losses are large compared to a closed system. Hence the efficient use of a desiccant system is also limited to large capacity refrigeration. Since the (closed-cycle) absorption system has no moving parts in its power cycle, low fluid velocities, and small irreversible heat transfer losses under low temperature conditions, the actual efficiency of this power cycle is closest to that of the Carnot power cycle.

Much research has been performed on the absorption refrigeration system, these works can be classified into two types; intermittent, Refs. (8,9,10,11), and continuous, Refs. (12,13,14,15,16,17). The continuous type uses a small amount of absorber but continuously circulates the working fluid (absorber and sorbent) between the absorber and generator. By using a heat exchanger the power cycle of the continuous type receives and rejects heat in a nearly reversible process (absorption or desorption process), while the absorber in the intermittent cycle is cooled and reheated alternately which causes some heat capacity losses during the absorption and desorption process. Thus the continuous

type more closely .approaches the theoretical efficiency of the Carnot power cycle than the intermittent type. .

For the continuous solar absorption cooling cycle, several working fluids have been studied, Refs. (12,14,16,17). Mansoori and Patel (18) have recommended NH(3)-water, NH(3)-NaSCN, and LiBr-water combinations as favorable candidates for the solar absorption cooling cycle. The LiBr-water pair is especially suitable in hot climates due to its low cost and excellent performance. One disadvantage for the LiBr-water combination is corrosion of the fabrication materials. Hydrogen is the product of this corrosive reaction; hydrogen increases the system pressure and thus lowers the COP of the cycle.

The most serious disadvantage of a continuous absorption cycle is that heat cannot be rejected easily by an air cooler on hot days. Hence an increase in the cost of the system results due to requiring a water cooling system for heat rejection. However the simple intermittent solar refrigerator can reject heat at a wider temperature range and only needs a simple and economic air cooler. Also the intermittent type broadens the cycle working temperature range to night-time temperatures which are favorable to the power cycle efficiency. By using the lower night-time

temperatures the refrigeration cycle efficiency is improved. In Figs.(2 and 3) it is shown that a high initial concentration of the sorbate (refrigerant) is imperative for both intermittent and continuous types to achieve a high overall system CP. A high sorbate concentration is achieved by maintaining the sorbent (absorber) at a low temperature. Due to the lower night-time temperatures, the intermittent cycle is more capable of accomplishing this requirement.

Since solar energy is low-grade but free energy, the cost of a solar refrigeration system will always govern the economic benefit. Because a low-cost air cooler can be used for heat rejection and the working temperature range can be broadened by the lower night time temperatures in the intermittent cycle, the solar-powered intermittent refrigeration system may have the possibilty of both lower system cost and good system performance.

For the intermittent refrigeration system, the system cost is a function of the system size. System size inturn strongly depends on the total latent heat of vaporization achieved in the evaporator. This total latent heat equals the total daily absorbed mass multiplied by its latent heat of vaporization. Thus the mass absorbed and its heat of

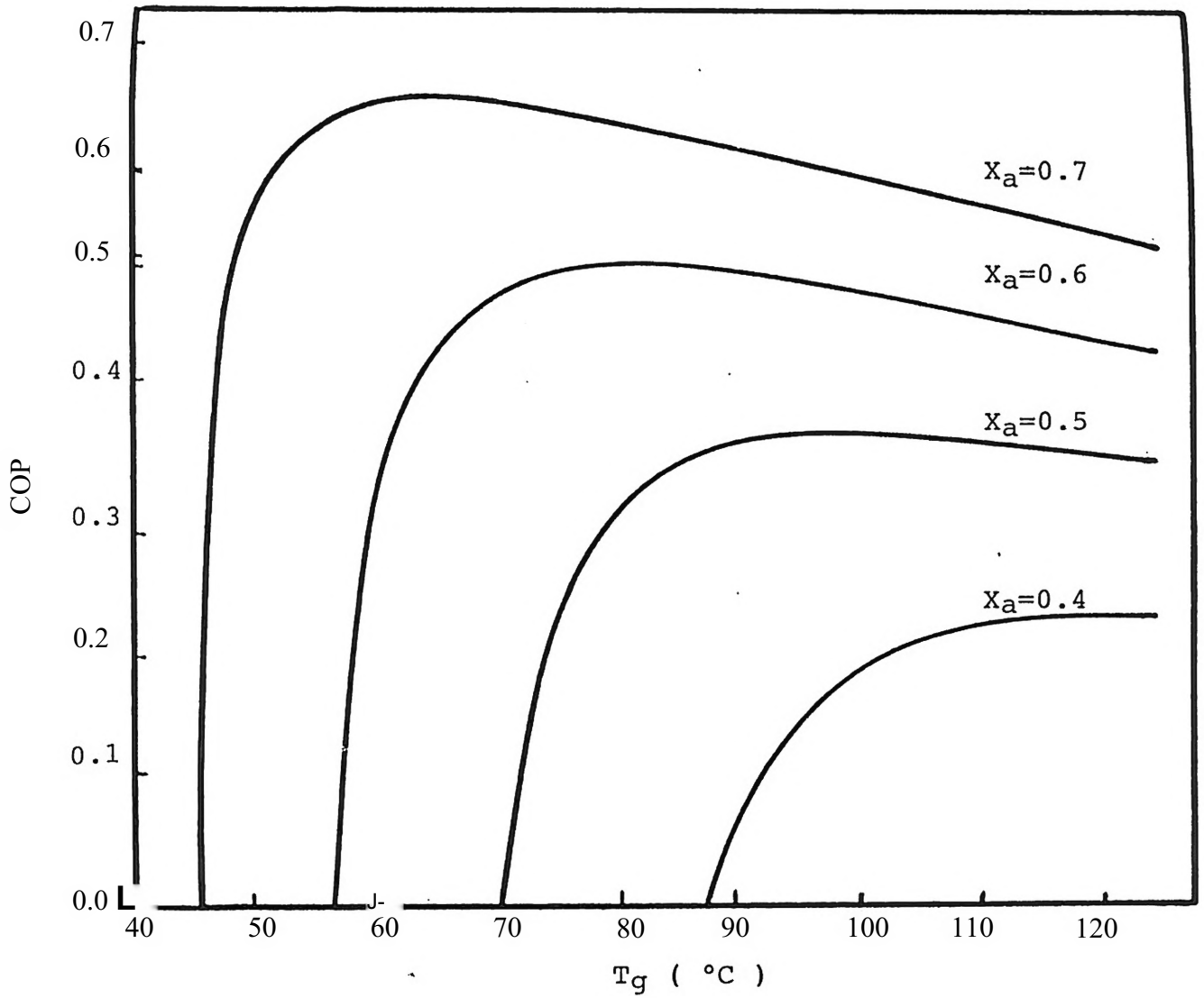

Fig. 2 Effect of Sorbate Concentration on COP (Ref. 8) Intermittent Type.

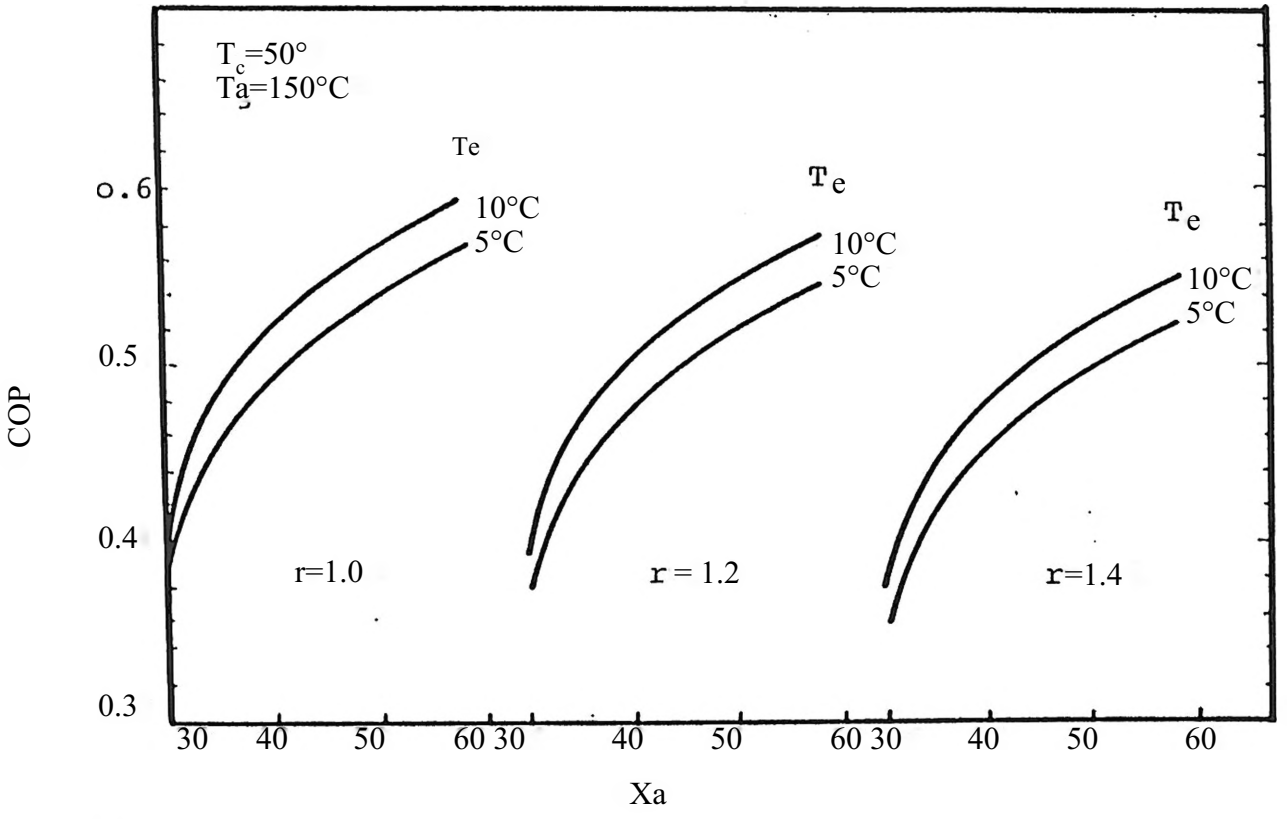

Fig. 3 Effect of Sorbate Concentration on (Ref. 15) Continuous Type.

vaporization are important factors affecting cost of the intermittent absorption refrigeration system.

Unlike the continuous absorption system, the intermittent system can use either a liquid or a solid absorber. The total daily mass absorbed and desorbed in the intermittent system is usually a small percentage of the absorber mass and depends on the absorption pair.

Typical isotherms for absorbed mass versus the saturated refrigerant vapor pressure is shown in Fig. 4 for:

(a) Microporous absorbents (zeolites, some carbons)

(b) Carbons, silica-gels,etc.

Comparing curves a and b of Fig. 4, it can be seen that the absorption isotherms for zeolites have a very weak pressure dependence. This weak dependence of mass absorption on pressure yields the ability of absorbing large quantities of refrigerant. Thus zeolites can be useful for application to solar intermittent refrigeration systems.

Zeolites can absorb a variety of refrigerants. Dubinin and Astakhov (19) have studied and discussed the limiting mass absorption values for some zeolite-refrigerent pairs. The daily water mass absorption for a simple solar-powered unit is about 5 to 10 weight percent of the zeolite. Tchernev (9) has pointed out that for most refrigerant gases the

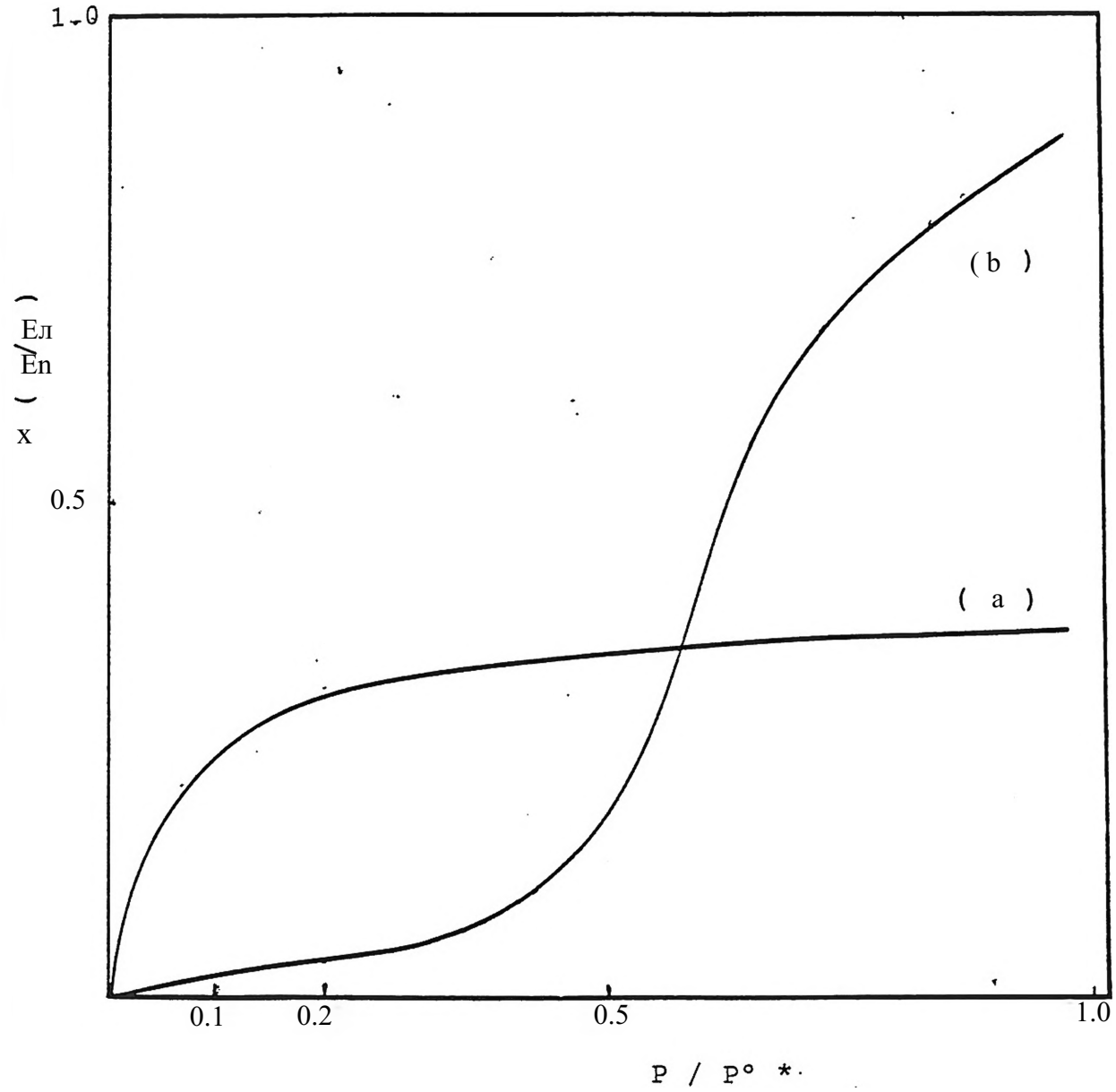

Fig. 4 Typici Isotherms for Absorbed Mass Versus the Vapor Pressure (Ref. 10).

* P is the Pressure above Absorber Fluid. P_σ is the Saturated Pressure Corrsponding to Temperature of Absorption.

maximum amount absorbed by a zeolite is about the same---------- 30 weight percent. The heat of vaporization for water is the highest of any common refrigerant, thus a zeolite-water pair was utilized in Tchernev[1]s refrigeration system.

In regard to the thermodynamic analysis, Guilleminot (20) was the first researcher to present a mathmatical model for zeolite refrigeration. He used a complex empirical correlation and experimental data to calculate the zeolite heat absorption value and system COP. Tchernev (9) experimentally determined the overall CP for a solar zeolite refrigerator but provided no analytical formulation. To compute solar absorption refrigeration system performance (CP), the refrigerant desorption temperature corresponding to the absorber temperature (collector working temperature) must be solved. Meuier and Mischler (10), treating the latent heat of vaporation as a constant, have solved the refrigerant desorption initiation temperature. Employing thermodynamic data for the zeolite(13X)-water pair, they presented a comparison between three pairs (LiBr-water, zeolite(13X)-water, and zeolite(4A)-water) as shown in Fig 5. They found that the zeolite(13X) was always better than the zeolite(4A). Among the three pairs the LiBr-water pair yielded the best performance for a heat sink temperture of 35 C. But, in the LiBr-water case, there was the difficult

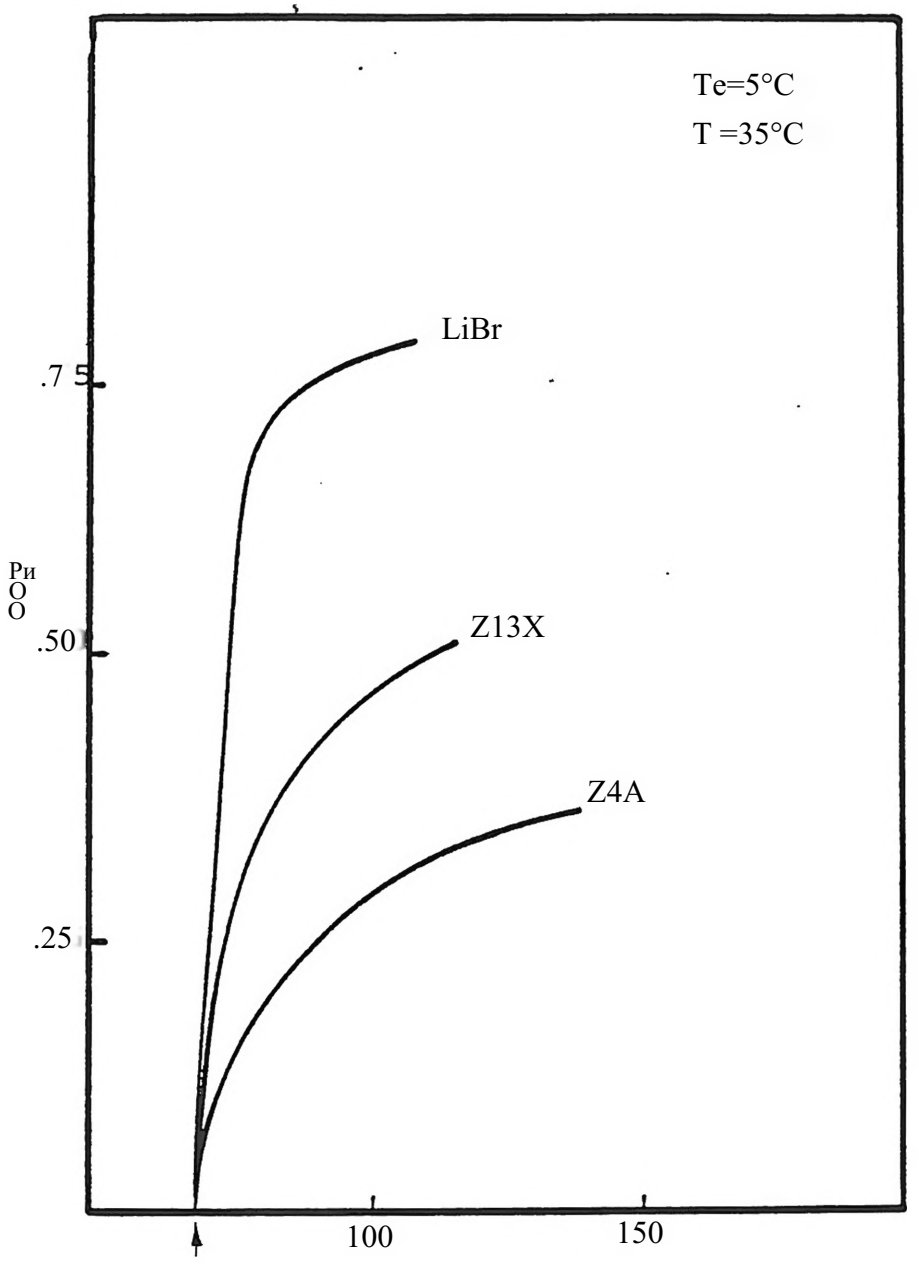

Fig. 5 Comparsoli of System COP for Three Absorption Refrigerators with Using Solar Energy. (Ref. 10)

problem of crystalization and as soon as the heat sink temperature reaches 45 C, the LiBr-water pair no longer functions. Thus the zeolite(13X)-water pair is best for the 50 C heat sink temperature. However, the initiation desorption temperature they computed is not realistic. The desorption initiation temperatures for different absorption pair are not the same even under the same operating condition (to be proved). But the desorption initiation temperatures of Ref.10 for these three pairs was given at the same point as indicated by the arrow in Fig 5. Therefore the system overall CP presented in Ref.10 must be corrected to account for the different desorption initiation temperatures. The conclusion that the zeolite(13X)-water pair was always better than zeolite(4A)-water pair should be reconsidered. In this work the effect of absorption pair properties on desorption initiation temperature has been considered, so that the desorption temperature for different working pairs can be solved correctly.

Meunier, Mischler, Cuilleminot and Simonot (11) noticed that the temperature at which zeolites begin to desorb water was very important for heat recovery during the absorption Phase. They designed a zeolite(13X)-water intermittent cycle and obtained some heat recovery from the heat rejection of zeolite during the absorption phase. Their

cycle allows more by-production (hot water) than Ref.(10) at the same time it provides cooling. They concluded that the zeolite(13X)-water pair produces a system overall CP of 0.33 with an evaporator temperature of 50 *C and a flat-plate solar collector generator temperature of 140 °C.

The works mentioned above .have all used zeolites inside a flat-plate solar collecor. Heat generated by the.solar collector was both transferred to the zeolite and loss to the outside ambient air. Heat loss to the outside air was significant due to the poor thermal conductivity of zeolite. ' However too much insulation of the solar collector, to reduce heat losses, can hurt the heat rejection required of the zeolite during the night cycle. In this work it was decided to employ a system which separates the zeolite from the solar collector so that it does not conflict with the night cycle heat rejection.

Seclecting the best type of zeolite is also important to the overall system CP. Most researchers noticed that the heat absorption value should be considered but few noticed that the desorption initiation temperature would strongly affect the solar-collector efficiency. Here a zeolite properties equation related to its heat absorption value and desorption initiation temperature has been derived. Using

this equation it can be shown how the system CP and heat absorption value will be affected by the slope of the constant mass line in a log Pv versus 1/Tz graph. An optimum system CP was determined by varying the constant mass line slope, the evaporation and condensation working temperatures, the ambient temperature, and the solar collector type. The results show: (1) The zeolite heat absorption value was determined by the slope of the constant mass line on a graph of' log Pv versus 1/Tz. (2) The system performance only shows a weak dependence on the heat of absorption when using a single glazing flat-plate solar collector. (3) The LiBr-water continuous cycle was found to have a slightly better performance but was also much more mechanically complex. (4) The zeolite intermittent cycle had slightly lower system performance than the LiBr-water system but had a wider operating range of heat rejection temperatures and could be used to simultaneously produce domestic hot water.

å

CHAPTER II

STATEMENT OF THE PROBLEM

Zeolites are natural and synthetic minerals made of silica and alumina. There are some 34 different varieties of natural zeolites which are found among volcanic rocks and in large clay deposits. The minerals contain microscopic pores and inner cavities which are very extensive. These inner cavities can virtually be empty when the minerals has been activated by heating. Although the crystal already contains metal cations which partially balance its electrostatic charges, the zeolite framework still carries a net charge which attracts polar compounds (polar compounds are molecules with relatively strong positively and negatively charged sites) such as water into the interior of the crystal. The diameters of the tunnels and pores running through the zeolite structure range from 3 angstroms (A) to about 10 A. This fits nicely with the kinetic dimeters of many chemicals. These pores and tunnels can absorb large quantities of water vapor (2.65 A), hence zeolites behave like a kind of solid absorber. Over a large pressure range zeolites can absorb or desorb water vapor as long as the zeolite is cooled or heated. Since the absorption or desorption proc-

ess is nearly independent of pressure, then by varying the temperature, zeolites can intermittently absorb water vapor from low pressure then desorb it at a high vapor pressure. The resulting effect is that zeolites function as a non-mechanical compressor.

A solar powered refrigeration system using the compression function of zeolites is illustrated in Fig. 6. There are two separate loops in the system. The left-side loop is composed of a sealed low vacuum tank filled with zeolite, a condenser, a water reservior, and an evaporator all of which have water vapor circulating within intermittently. The right-side loop has a heat transfer fluid circulating within a closed loop composed of a heat exchanger coil in the zeolite tank, a pump, a solar collector, and an air cooler. The left-side loop is in an evacuated state (5 mm- 50 mm Hg) while the right-side loop is at normaL (approximately atmospheric) pressures.

In the day-time cycle (switch at day-time position shown in Fig.6) the solar energy recieved by the solar collector will transfer heat to the zeolite through the right-side loop. The heat transfer fluid in the right-loop absorbs heat from the solar collector and then transports this heat to the zeolite. After leaving the zeolite tank,

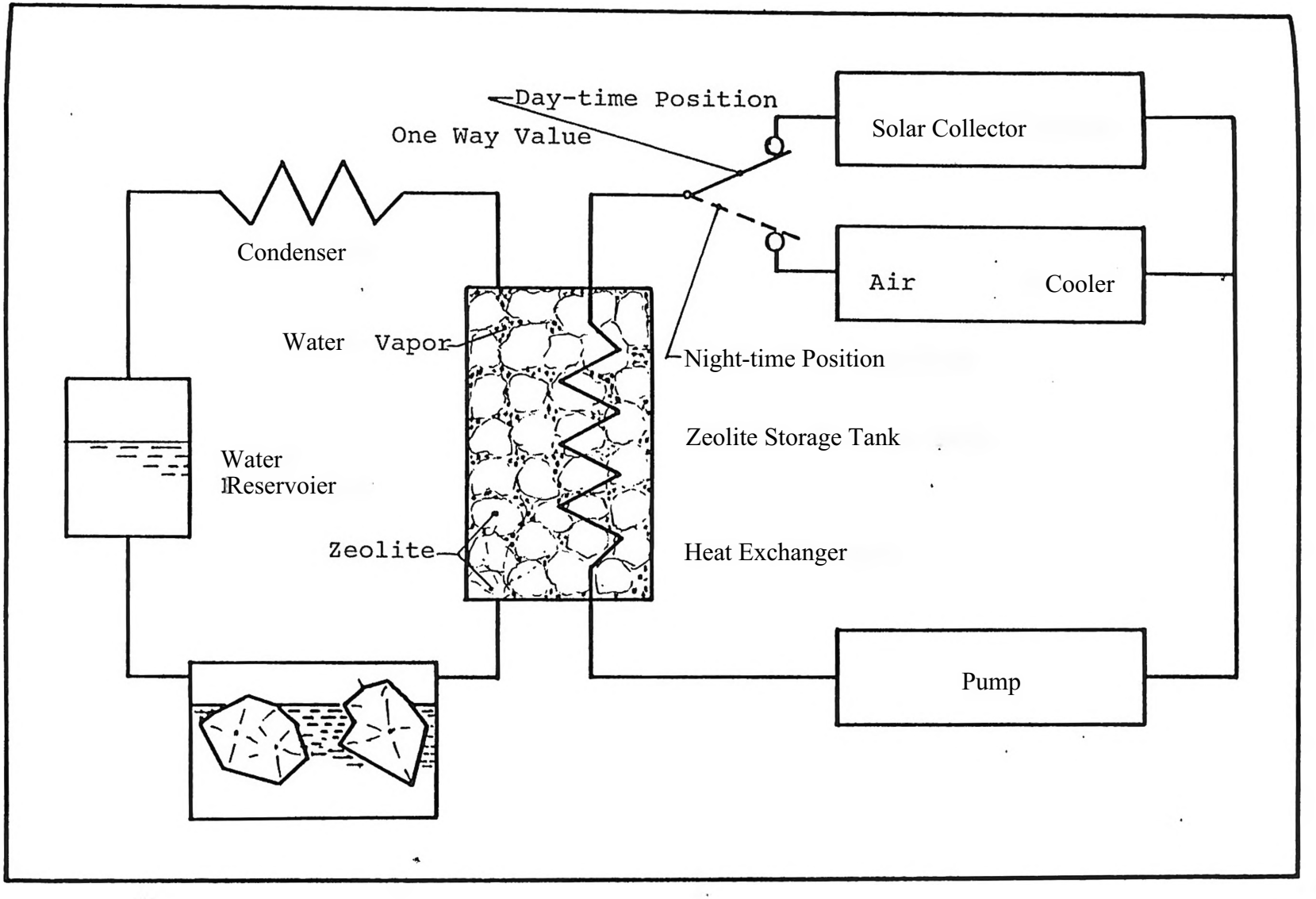

Fig. 6 The Solar Zeolite Absorption Refrigeration System

the heat transfer .fluid is again pumped to the solar collector to absorb more heat and again bring this heat to the zeolite tank. The zeolite, being heated, desorbs water vapor to the condenser (left-side). The vapor pressure then increases until reaching the state where the water vapor temperature is higher than the ambient fluid outside the condenser. The water vapor then condenses and drains into the water reservior after its latent heat of condensation has been released to the ambient fluid outside the condenser. Thus domestic hot water or a heating effect can be obtained from the condenser during the day.

During the night-time cycle (switch at night position shown in Fig.6) the zeolite is cooled by the outside ambient air through the right-side loop. At night the air cooler is used to transfer heat from the zeolite to the cool night air. Being cooled, the zeolite absorbs water vapor from the evaporator (left-side). As water vapor is absorbed the vapor pressure decreases . As the vapor pressure decreases to about 0.1 psia (5 mm) the water in the evaporator will vaporize (boil) and likewise absorb heat from its outside medium, thus the cooling effect can be produced from the evaporator during the night.

The above system is only a simple example for showing the principle of the heating and cooling effect in the solar-powered zeolite intermittent refrigeration cycle. Significantly more complicated systems can be designed. Since the solar energy is provided only during the day, a cooling and heating storage capability is needed in the intermittent absorption refrigeration system for handling the cooling or heating load of the entire day or for several cloudy days. The hot storage tank is used to receive the heat released by the condenser in the left-loop. At the end of the day-time cycle (4:00 P.M.) hot water is available in the hot storage tank. Thus domestic hot water is produced in this system and about the same amount of heat is added to the water as for the simple solar collector. The by-product (hot water) will be continuously produced during the day-time cycle.

The cold storage tank is designed such that it can be cooled by the evaporator. During the night, ice is produced in the cold storage tank. During the day the ice, which was formed during the night, in the storage tank will slowly melt but maintain the refrigerated space at a constant low temperature. The melted water in the cold storage tank will be cooled to ice again during the next night-time cycle.

The system based on the heat of absorption value of 1800 BTU/lbm (to desorb 1 lbm of water out of zeolite requires 1200-1800 BTU), and assuming the total daily incident solar energy to be 1800 BTU/ft2 (approxmately 900 BTU/ft2 is converted into heat energy), the total daily water desorbed will be approxmately 0.5 lbm/ft2 of solar collector. For most zeolites the differential water loading is about 5 percent by weight between ambient temperature and 250*F, thus the total zeolite weight will be about 10 lbm/ft2 of solar collector. Because 1 lbm of water vaporization (heat of vaporization is 540 BTU/lbm) will produce about 7 lbm of ice (heat of melting is 80 BTU/lbm) the size of the cold storage tank at the evaporator will be about seven times larger than the total daily water desorbed from the zeolite. The cooling effect will be about 360 BTU/ft2 assuming the system CP to be equal to 0.2. The physical problem defined in this chapter will now be thermodynamically modeled to determine the the quantitative and qualitative dependence of the system CP on the various governing parameters.

CHAPTER III

THERMODYNAMIC ANALYSIS

3.1 System Performance Based on Carnot Cycle

In Chapter II it was shown (Fig.1) that the use of solar energy to produce cooling via a vapor-compression cycle required three steps of energy conversion. The relationship between the system overall CP and these three energy conversion factors can be expressed as

$$CP = COPr \times {}^{\wedge}P \times co \quad \eta \qquad (1)$$

where CP is defined as the ratio of the cooling effect to the total incident solar energy, ^Z^is the efficiency pf the solar collector at step 1, p is the efficiency of the power cycle at step 2, and COPr is the coefficient of performance for the refrigeration cycle at step 3.

The conversion efficiencies between the work and heat at step 2 and step 3 (Fig.1) are governed by the second law of thermodynamics. The limiting efficiencies of these energy conversions between two given temperature limits can be

calculated from the Carnot cycle. These ideal efficiencies are given by

$$\eta_C = (T_H - T_L)/T_H \quad (1a)$$

$$COPr = T_U/(T_H - T_L) \quad (1b)$$

where (see Fig.7) T_H of the Carnot power cycle will be the generator temperture (Tg) and the low working temperature T_L will be the ambient temperture (T_w). The values T_H and T_u of the reverse Carnot cycle will be the ambient temperature, T«, and the evaporator temperature, Te, respectively. Combining these terms yields the system overall CP from Eq.(1) as

$$CP_C = (\hat{2}) \times \eta_g \cdot \frac{T_e}{T_\infty - T_e} \times 7_{CO} \quad (2)$$

Equation(2) can be applied to all kinds of solar vapor-compression refrigeration systems. The T-s diagram related to Eq.(2) is shown in Fig.7b.

3.2 Refrigeration Cycle

For the absorption refrigeration system, the working temperature range in Eq.(2) must correspond to the

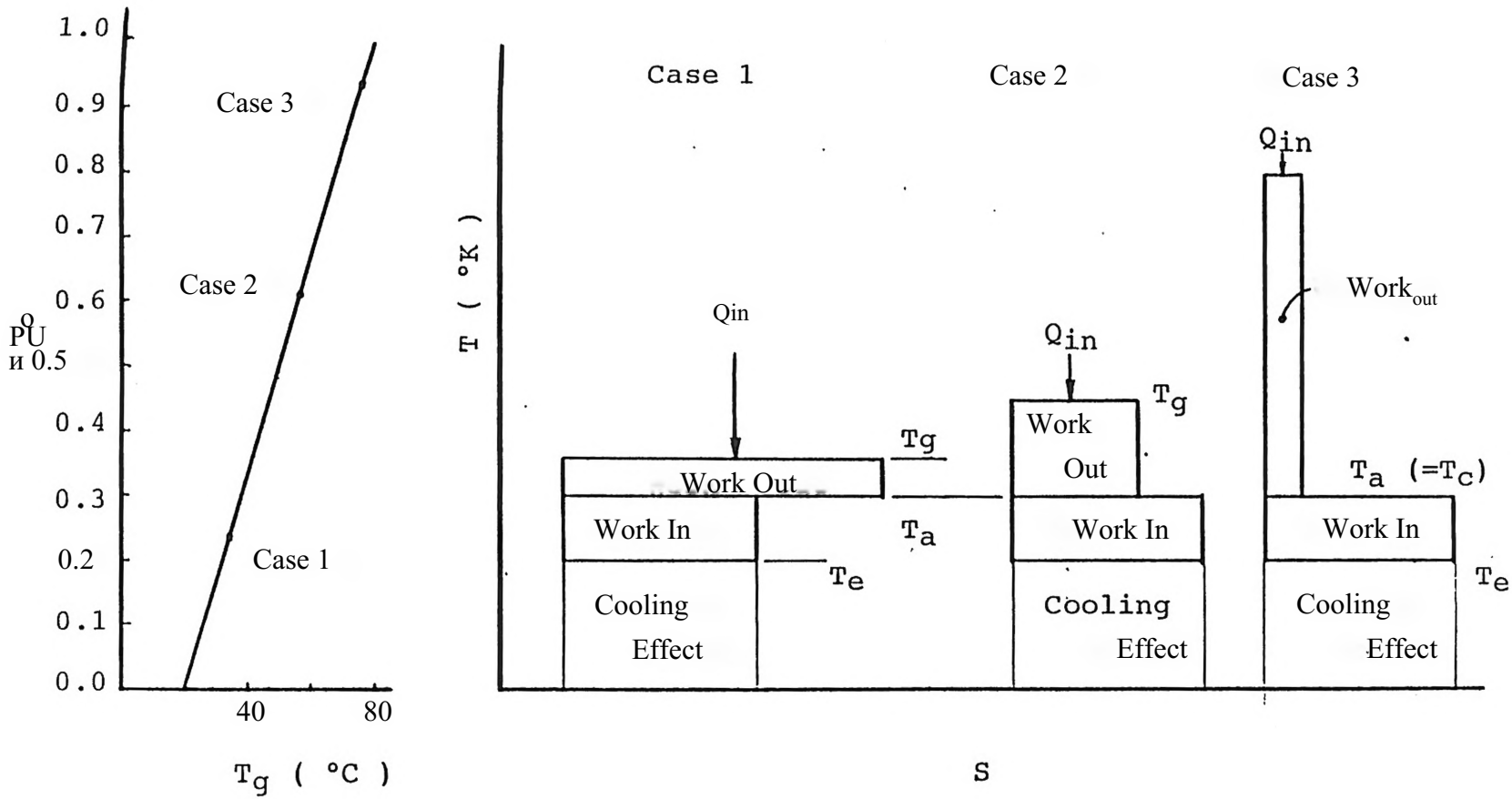

(a) CP_c Versus Tg

(b) T-s Diagram

Fig.7 T-s Diagram Illustrating Syatem Overall Performance, CP_c, as a Function of Tg.

absorption cycle., As mentioned in the statement of the problem, the working fluid of the absorption cycle is the vapor desorbed from the absorber. The vapor properties at each specific point in the cycle can be illustrated by a T-s diagram as in Fig.8. Figure 8a shows the flow chart of the absorption refrigeration system. The refrigerent (water vapor) temperature versus absorber temperature is shown in Fig.8b. The T-s diagram related to this system is shown in Fig.8c. It should be noticed that the absorption and desorption processes occur at different temperatures Tai and Tgi (which are determined according to their instantaneous mass concentration, Xi as shown in Fig.8b). However, the absorption and desorption processes can be classified as many pairs which (each pair of absorption and desorption processes) has a fixed sorbent mass concentration. Assuming the temperature of the zeolite inside the storage tank is uniform, then at any instant the zeolite will be at some mass sorbent concentration Xi, at which a given evaporation and condensation pressure yields two corresponding absorption and desorption temperatures Tai and Tgi (Fig.8b). The desorption and absorption processes under this instantaneous mass concentration were indicated by lines 1-2 and 7-1' (shown in Fig.8c) respectively. It can be seen that the refrigeration cycle is marked 3-4-5-6, while the power cycle

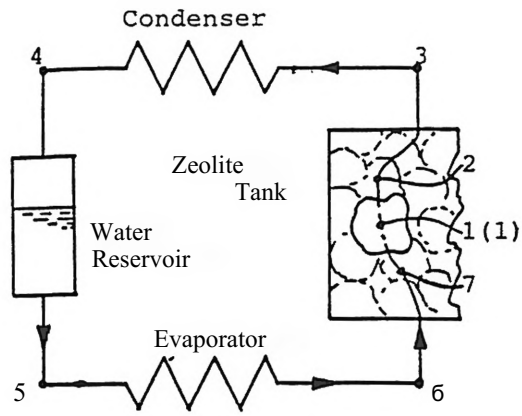

(a) Refrigerant Flow Chart

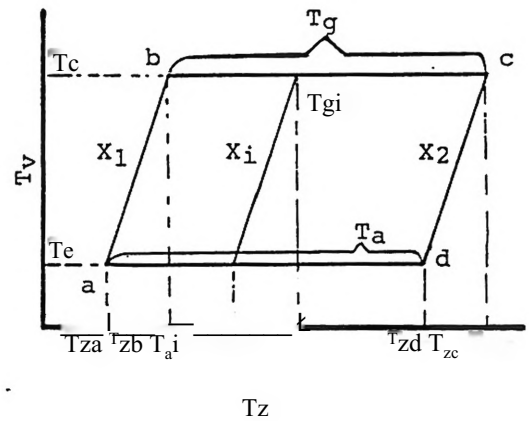

(b) Temperature Relation between Refrigerant(Tv) and Absorber (T_z)

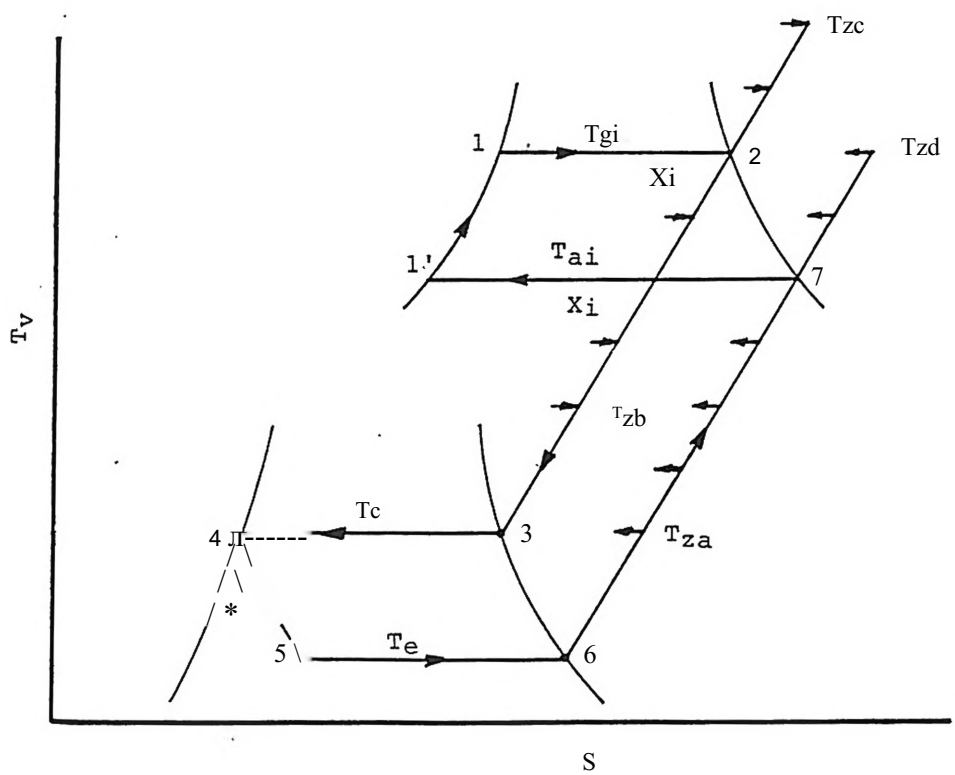

(c) T-s Diagram of Water Vapor (Refrigerant) Corresponding to Figs. (8a) and (8b).

Fig. 8 Relationship between Absorption Properties and Absorption Refrigeration Cycle.

is marked by 7-1'-1-2. The maximum system CP (according to the Carnot cycle) has been presented in Eq.2 and Fig.J.

As seen, for the absorption cycle,the working temperature range in the power cycle is limited by the absorption and desorption temperature range (as indicated by Ta and Tg respectively in Fig.8b). Due to the relationship between the instantaneous absorption and desorption temperatures (as indicated by Tgi and Tai in Fig.8b), the desorption temperature must increase as the absorber temperature increases. Hence the working temperature T_L (=Ta) of the power cycle must also increase. Therefore the instantaneous Carnot cycle CP for the absorption working temperature can be written as

$$CP_{ca} = \left(\frac{T_g - T_a}{T_g} \right) \times \eta_{H?'' X} \times o^{1} e \qquad (3)$$

Equation(3) is based on the Carnot cycle, but the working temperature range is limited by the absorption temperature range (Tgi and Tai in Fig.8b). Figure 9a shows a T-s diagram corresponding to Eq.(3)· It is seen from Fig.9a that the power cycle has a reduced net amount of work (area c) when compared to Fig.7· However, the area C will decrease to zero as Tai approached to T_{∞}, which means Eq.(2) and Eq.(3) have the same CP at point P (Fig.9b). Since the

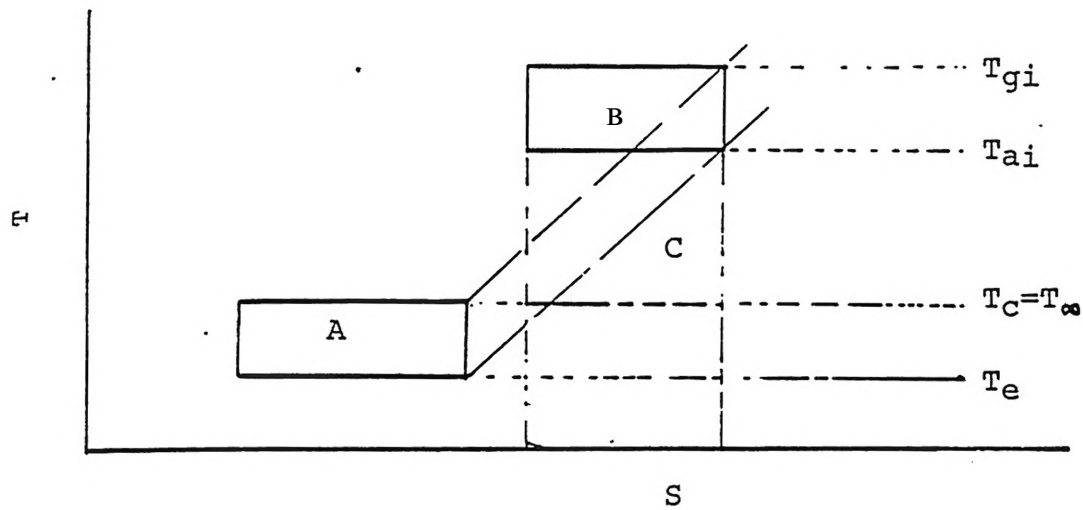

(a)T-s Diagram

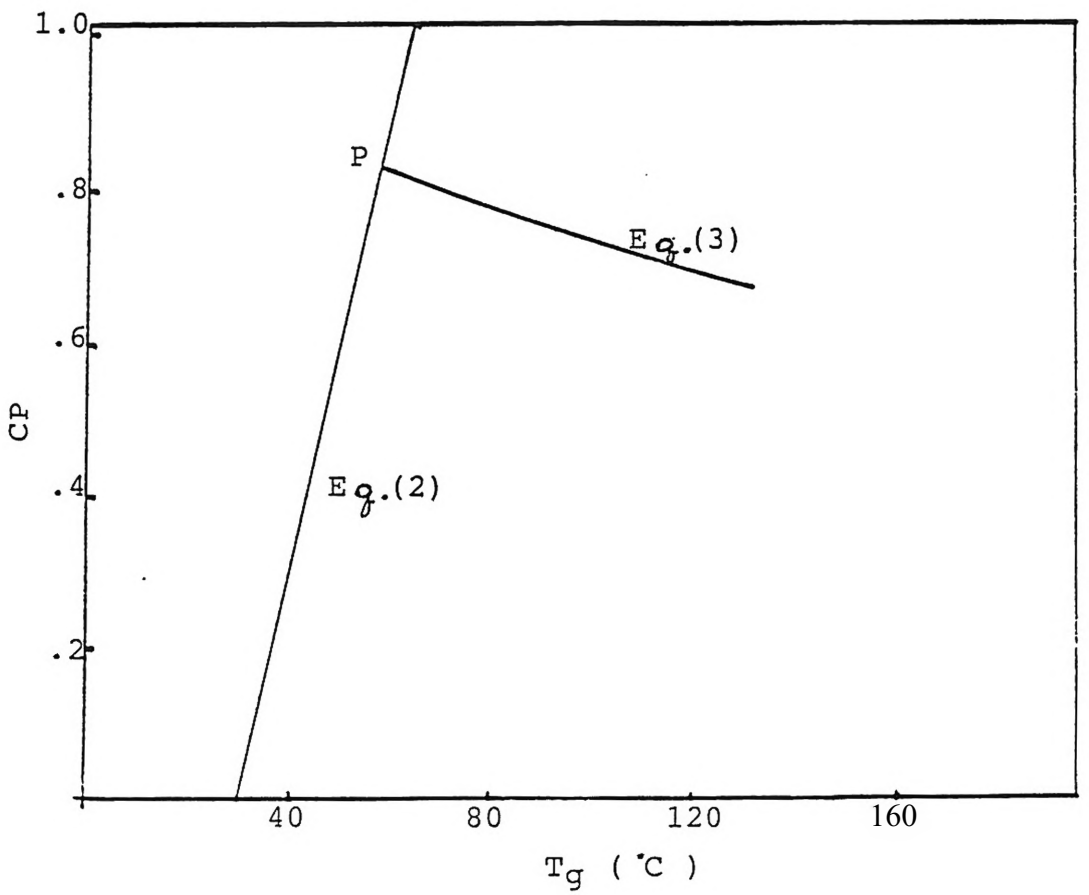

(b) CP Versus Tg

Fig. 9 Comparison of two Carnot Refrigeration Cycles

(1) Power Cycle (T^T^) (2) Power Cycle ($T_L=T_{ai}$)

area A must be equal to the area B, then as Tg increases, Ta must also increases. This condition yields a net work loss (area C) which causes the system CP to decrease from point P ($Tai = T_{OT}$). Thus the system CP (Eq.(3)) will decrease for Tai > T«, (Tg > Tp); this is shown in Fig. 9b.

To consider the phase transformations involved in the absorption-desorption processes of the above case, a more realistic limitation for the system CP can be derived by employing the Clausius-Clapreyon relation for the phase transformations. For an absorption system, the theoretical overall CP can also be expressed as follows

$$CPa = COPr \times 7pa \dot{x} \hat{}co \qquad (4)$$

By the defenition of COPr and ^p this can be written as

$$CP_{a} \text{ - } \frac{\text{Work Out}}{(Q_{in}} \times / \frac{\text{Cooling Load}}{\text{Work in}} \hat{X} \hat{}co \qquad (5)$$

Since the work output of the absorption power cycle must be equal to the work input to the refrigeration cycle, Eq.(5), reduces to

$$cp_a = \frac{\text{Cooling Load}}{\text{y1II}} \times 7co \qquad (5a)$$

The cooling load will be equal to the latent heat of vaporation, L, in the evaporator. The heat input, Qin will be equal to the heat absorption value, ΔH, in the absorption process. Thus the overall absorption system efficiency considering the phase transformation in absorption process becomes

$$CP_a \quad \frac{L}{\Delta H} \quad {}' x \wedge co \qquad (ð)$$

As seen in Fig.8b, the heat absorption' process occurs between the evaporator pressure (Pe) and the condenser pressure(Pc). The heat absorption value ΔH, corresponding to the above pressure changes, can be determined from the Clausius-Cl apreyon equation for an equilibrium phase transformation. Hence applying the Clausius-Clapreyon relation to the vapor-solid transformation yields

$$d(\ln P)/dT = \Delta H/RT^2 \qquad (6a)$$

Integration of Eq.(6a) between Pe (Ta) and Pc (Tg) of Fig.8b yields

$$\ln(Pc/Pe) = \int_{Tat}^{T9} K\,\Delta H/RT\,)\,dT \qquad (6b)$$

for the liquid-vapor transformation in the evaporator the Clausius-Clapreyon relation can be written as

$$d(\ln P)/dT = L/RT^2 \qquad (6c)$$

Integration of Eq.(6c) between Pe (Te) and Pc (Tc) of Fig. 8b yields

$$\ln(P_c/P_e) = J(L/RT^2)\, dT \qquad (6d)$$

Combining Eqs. (6b) and (6d) gives the result

$$f_L\, d(-i-) = J_{AH}\, d(-i-) \qquad (6e)$$

Taking L and AH as constants in Eq.(6e) yields

$$L\,(1/Te - 1/Tc) = AH\,(1/Ta - 1/Tg) \qquad (7)$$

Rearranging Eq.(7) to find L/ΔH and combing with Eq.(6) gives

$$CPa = \frac{T_g - T_a}{T_g} - (\text{illegible}) \qquad (8)$$

Combining Eqs.(3)$_i$and (8) produces a relationship between the overall Carnot cycle CP (based on the absorption .working temperature) and the absorption cycle CP as follows

$$CPa / CPc = Tc / Ta \qquad (9)$$

Equation(9) shows that the performance of the absorption cycle is very close to the Carnot cycle when Tc is close to Ta (typically $0.9 < Tc/Ta < 1.0$). The T-s diagram involving the absorption process has been shown in Fig.8c. It should be noticed that the power cycle receives and rejects heat at the same heat of absorption, ΔH, value (the proof will be shown in Eq.(14)). Since Qin is equal to Qout, according to the first law of thermodynamics there is no net work output from the power cycle. However, from the second law of thermodynamics, the theoretical maximum net work output of the power cycle for this case is equal to the net decrease ,of the avaiablity between the heat of desorption and heat of absorption, this is shown in Fig.10.

Figure 10 shows that the power cycle of the absorption system has Qin at Tgi (desorption process), and has Qout at Tai (absorption process). The net work produced will be equal to the net decrease of availability between the energy

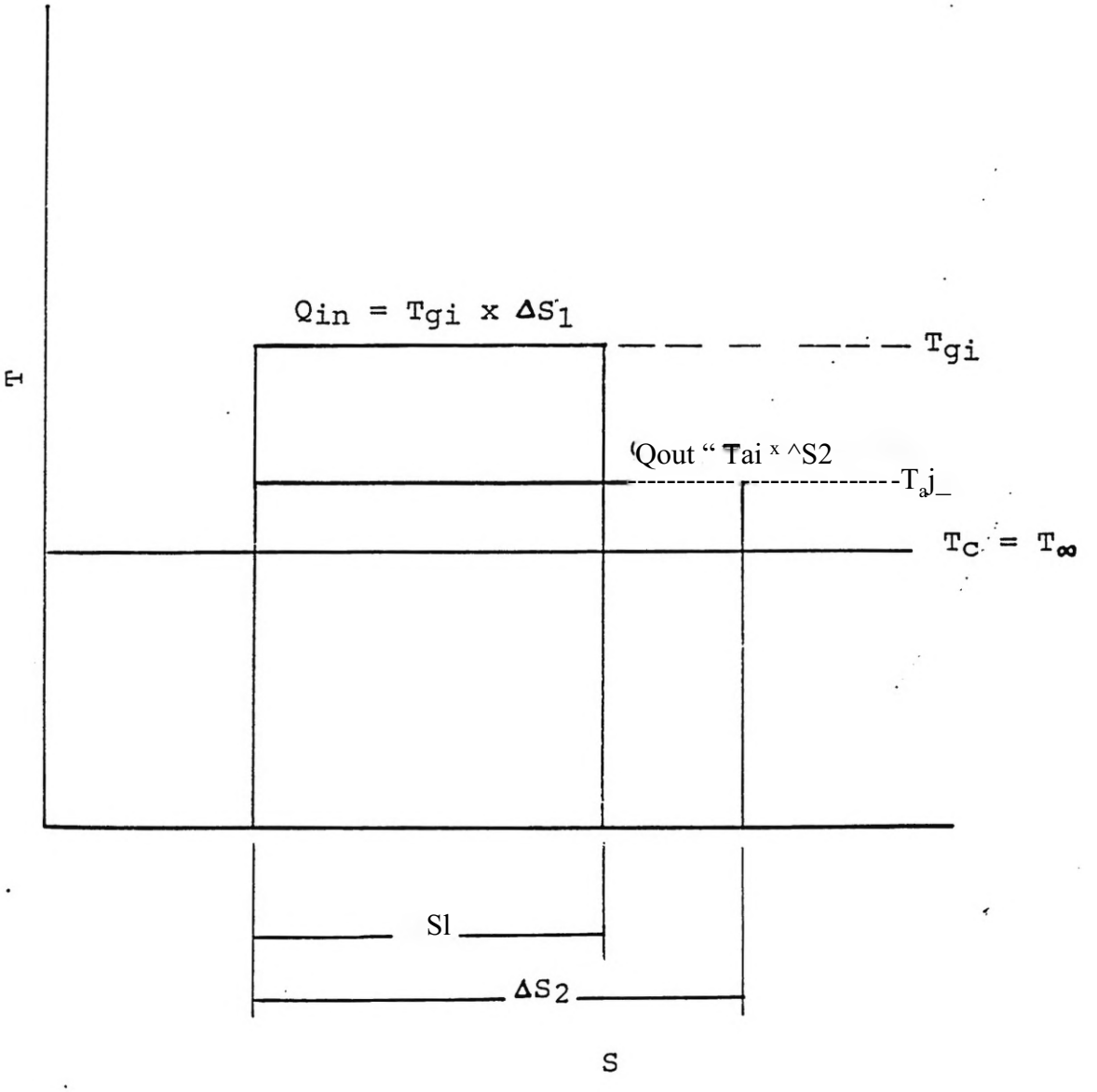

Fig.10 T-s Diagram to Illustrate Maximum Work of The Power Cycle in Absorption Refrigeration System.

in and the energy .out, which is TC(AS2-AS1) (see Fig.10).

Thus the power cycle efficiency is given by .

$$\eta_a = \frac{\text{Work Net}}{Q_{in}} = \frac{T_c \times (AS_2 - AS_1)}{Tg \times AS_i} \quad (10)$$

Since the heat of absorption (Q in) is the same as heat of desorption (Q out) under the same mass concentration, then

$$Tg \times S_I = Ta \times AS_2 \quad (10a)$$

Combining Eqs.(10) and (10a) yields

$$\eta_a = \frac{T_c}{T_a} * \left(1 - \frac{T_a}{Tg}\right) \quad (10b)$$

Under the same conditions, the efficiency of the Carnot cycle based on the absorption system working temperatures will be .

$$\eta_c = 1 - \frac{T_a}{Tg} \quad (10c)$$

Combining Eqs.(10b) and (10c) yields

$$\frac{\eta_a}{\eta_c} = \frac{\eta_a}{T_c} \quad (10d)$$

This leads to

$$-\frac{CPa}{CPc\ T_c} = -b \qquad (10e)$$

Equation(10e) was derived from the T-s diagram (see Fig.10) based on an absorption process involved in the power cycle, Comparing Eqs.(10e) and (9) shows that they are the same, thus indicating agreement between the T-s diagram and the phase transformations approach using the Clausius-Clapreyon equation. According to Eq.(10e), the T-s diagram for the absorption cycle will look like Fig.11a.

Figure 11a shows that the absorption process (of the power cycle) has the effect of decreasing the net work (by an amount equal to area C). This decrease of net work can be calculated from Eq.(10b). Figure (11b) shows that Eq.(8) is very close to Eq.(3) and both equations intersect at point P (where Tai=Too,· Tg and Ta are the corresponding absorption and desorption temperatures for mass concentration Xi). These results agree with Eq.(10e) and Eq.(9). Equation(8) provides an instantaneous overall system CP for the absorption cycle. This is valid for all solar absorption refrigeration systems. The disadvantage of Eq.(8) is that measurements of Tai and Tgi are required to determine the instantaneous performances. Fortunately, the relation

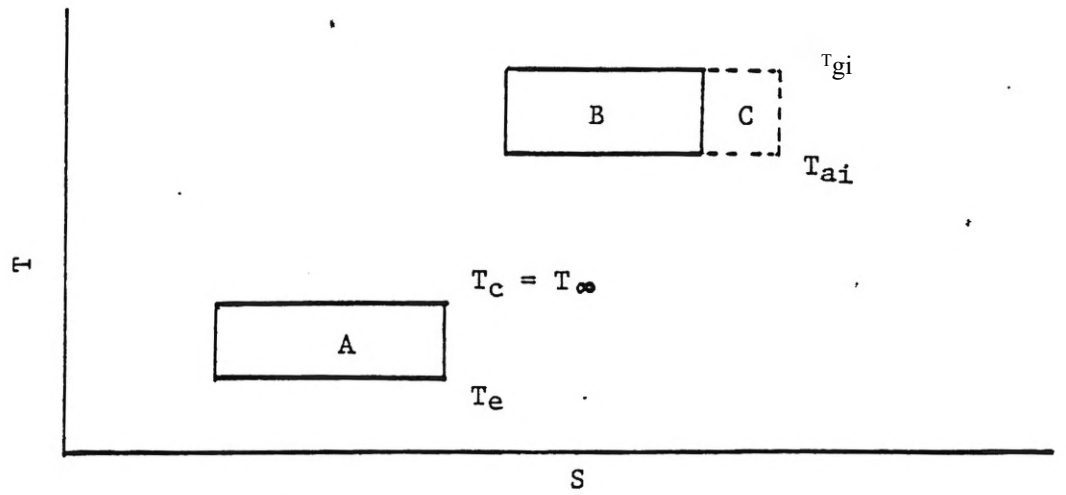

(a) T-s Diagram

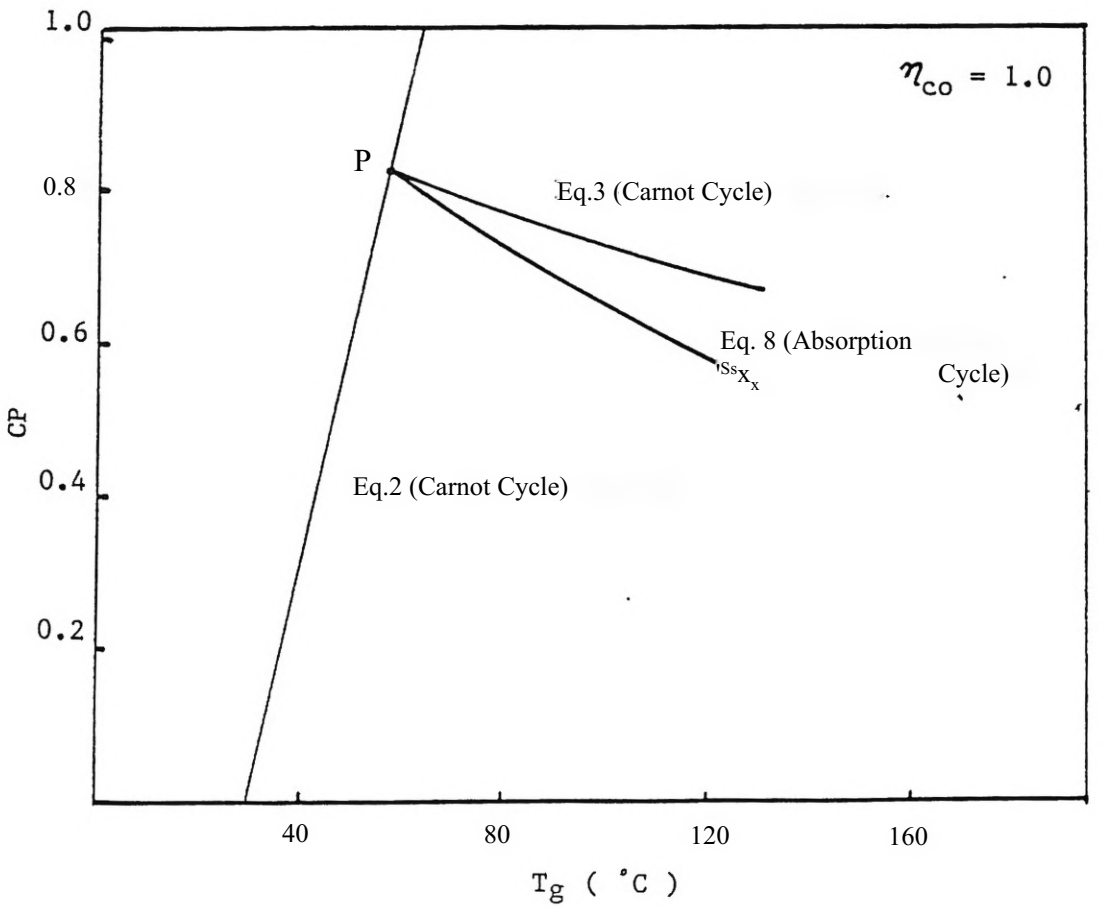

(b) CP Versus Tg

Fig. 11 Comparison between Carnot Cycle and Absorption Cycle.

between Tai and Tgi can be derived from the absorber properties; this derivation is presented in the following section.

3.3 Absorber Properties EcLuation

To derive a simple absorber properties equation related to the absorption process it was assumed that the constant mass absorption line was linear in the coordinates of log Pv versus 1/Tab. It was shown by Dubinin and Serpinsk (21) that the linearity of the isosters (Fig.12) is in agreement with the theory of volume filling of microporous absorbents (such as zeolite). The results from Ref.21 showed the strong linearity of the constant mass lines and are illustrated in Fig.12. Under the linearity assumption (as verified by Fig.12), the absorber properties relation can be expressed as

$$\log P_v = m \times (\zeta\psi\text{^-})^{+c} \qquad (11)$$

Equation (11) is a general form of the absorber properties relation. To apply Eq.(11) for computing Ta and Tg it is necessary to differentiate Eq.(11) and write it in the following form

$$m = \frac{-d \log Py}{d\,(1/Tg)} \qquad (11a)$$

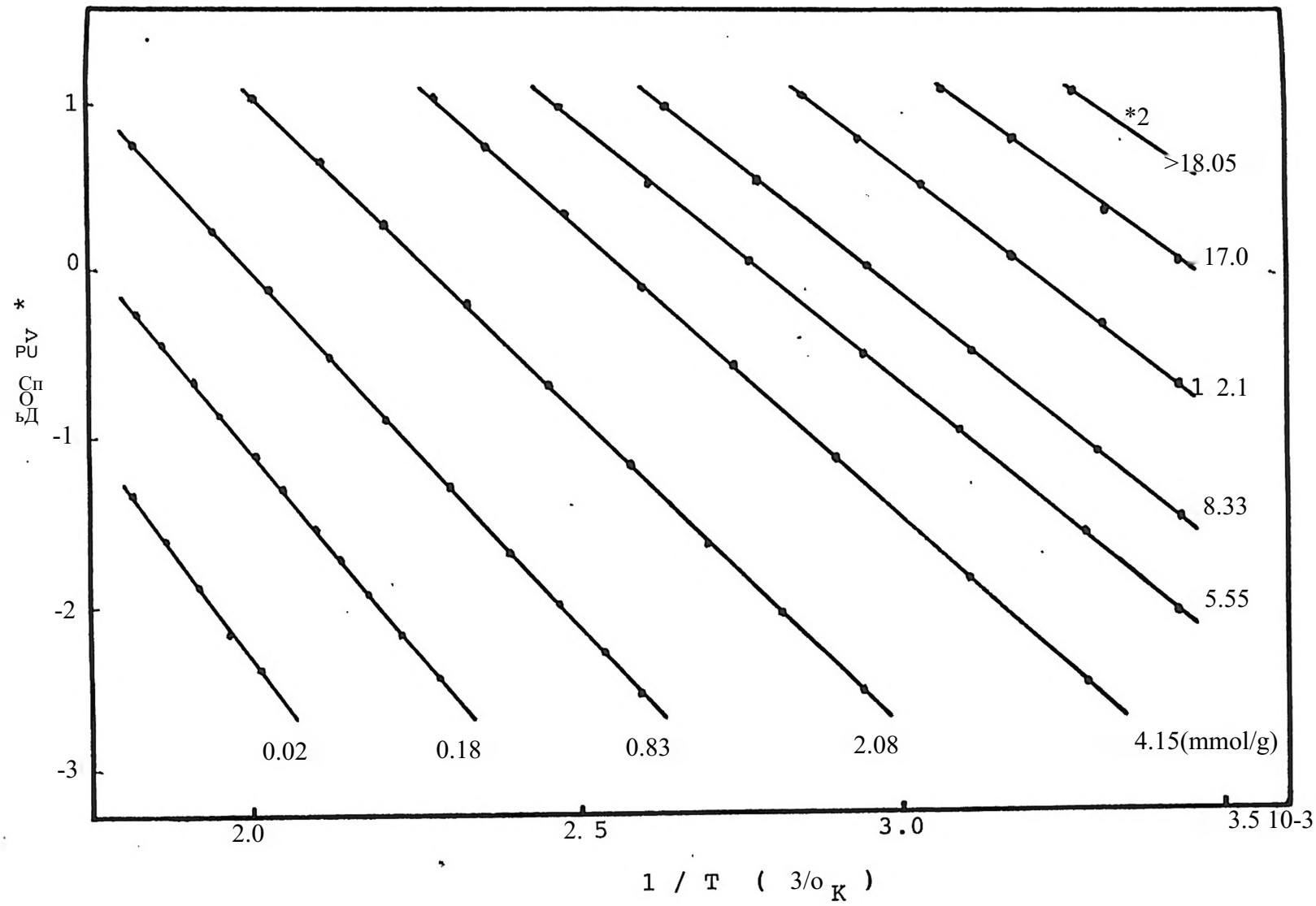

Fig. 12 The Log P_v Versus VTQ Plot for Zeolite NaX-Water Pair from Experimental Data. (Ref.21)

* P_v (mmHg)

Now Eq.(6a) can be rewritten as

$$\frac{\Delta H}{R} = \frac{2}{T} \times \frac{d \ln P}{d(1/T)} \times \frac{d \ln P}{-T^{\wedge} d(1/T)} \qquad \text{d log P} \qquad (no)$$

Simplification of Eq.(12) yields

$$\Delta H = R \quad \frac{-d \log P}{d(1/T)} \quad z \, A \frac{\ln *}{d \log P} \qquad (13)$$

Combining Eqs'. (11) and (13) gives the expression for ΔH as

$$H = Rme \left(e = \quad \log \overset{*}{P} \quad \right) \qquad (14)$$

This expression shows that the heat absorption value, ΔH, is only a function of the slope, m, of the constant mass line on a log Pv versus 1/Tab plot. All the points along a given constant mass line have the same slope (Fig.12). Therefore each point along the same constant mass line has the same heat absorption value, ΔH. Hence from Eq.(14), a line of constant heat absorption will also be a line of constant mass absorption.

3·4 atio^shen AbS.Oi Lp b^r and Abs.^nhâțe Iemas.Iiatuiie

(a) Assuming Constant Heat of Vaporation

Using Eq. (11) for the absorber one can write

$$\log P_v = m\,(-¿-) + C_{ab} \qquad (15)$$

This equation represents all the constant mass lines (hence also the constant heat-absorption lines), where Pv is the equilibrium vapor pressure abov.e the absorber and Tab is the temperature of the absorber at this vapor pressure. To change the coordinates from Pv versus 1/Tab to Tv versus 1/Tab , it is necessary to know the relationship between Pv and Tv. To determine this relationship the Claperyon equation is employed between the phase equilibrium state of the liquid and the vapor; therefore from Ref. 22, the Claperyon equation can be written as

$$\frac{d\,P_v}{d\,T_v} = \frac{L}{T_v \times (V_v - V_f)} \qquad (16)$$

Using the ideal gas equation of state for the vapor and realizing that v^ « v_v , Eq.(16) becomes

$$\frac{d\,P_v}{P_v} = L \times \frac{d\,T_v}{R\,T_v^2} \qquad (17)$$

Now from Eqs.(6a) and (14) for the absorber it can be written

$$\Delta H = Rme = RTaL2\ X \frac{V^{*}\cdot P_v}{d\ T_{ab}} \quad (18)$$

Using the ideal gas equation of state again and simplifying yields

$$Rue = RT_{ab}^2 \times (\text{—}^{\wedge}\text{-}) \times (d\ P_v) \times \frac{1}{d\ T_{ab}} \quad (19)$$

An expression for dPv can be obtained from Eq.(17); combining Eq.(17) with Eq.(19) gives the result

$$Rme = \frac{T_{ab}^2 \times L \times d\ T_v}{Tv^2 \qquad d\ T_{ab}} \quad (20)$$

Separating the variables now produces

$$\frac{d}{T_V^2} = \frac{Rme}{L} \times \frac{d\ ^{\wedge}ab}{Tab^2} \quad (21)$$

in reality the value L for water is a very weak function of temperature, hence L was taken as constant and Eq.(21) was integrated giving the result

$$1/T_V = \frac{Rme}{L} \times (1/T_{ab}) + C \quad (22)$$

or

$$T_V = \frac{1}{\frac{Rme}{L} X \quad (1/Tab) + \quad c} \quad (23)$$

Equation (23) shows the relationship between absorber and absórbate temperature based on a constant heat of vaporation. The relation in Eq.(23) is plotted in Fig.13 to show the essentially linear relation between Tv and Tab.

(b) Based on Heat of Vaporation
Being a Function of Temperature

Equation (23) is based on the assumption that the latent heat of vaporation is constant over the integration temperature range. However, the latent heat of vaporation does vary slightly with temperature. Using Eq.(23) to compute the absorption or desorption initiation temperatures may cause some inaccuracy (to be shown in Fig.16). To avoid this inaccuracy (or to make the equation more applicable over wide temperature range) an alternate form of Eq.(23) was developed by allowing the latent heat of vaporation to be considered as a linear function of temperature. For the zeolite-water pair this functional dependence can be written for water as

$$L=mLXTv + CL \qquad (24)$$

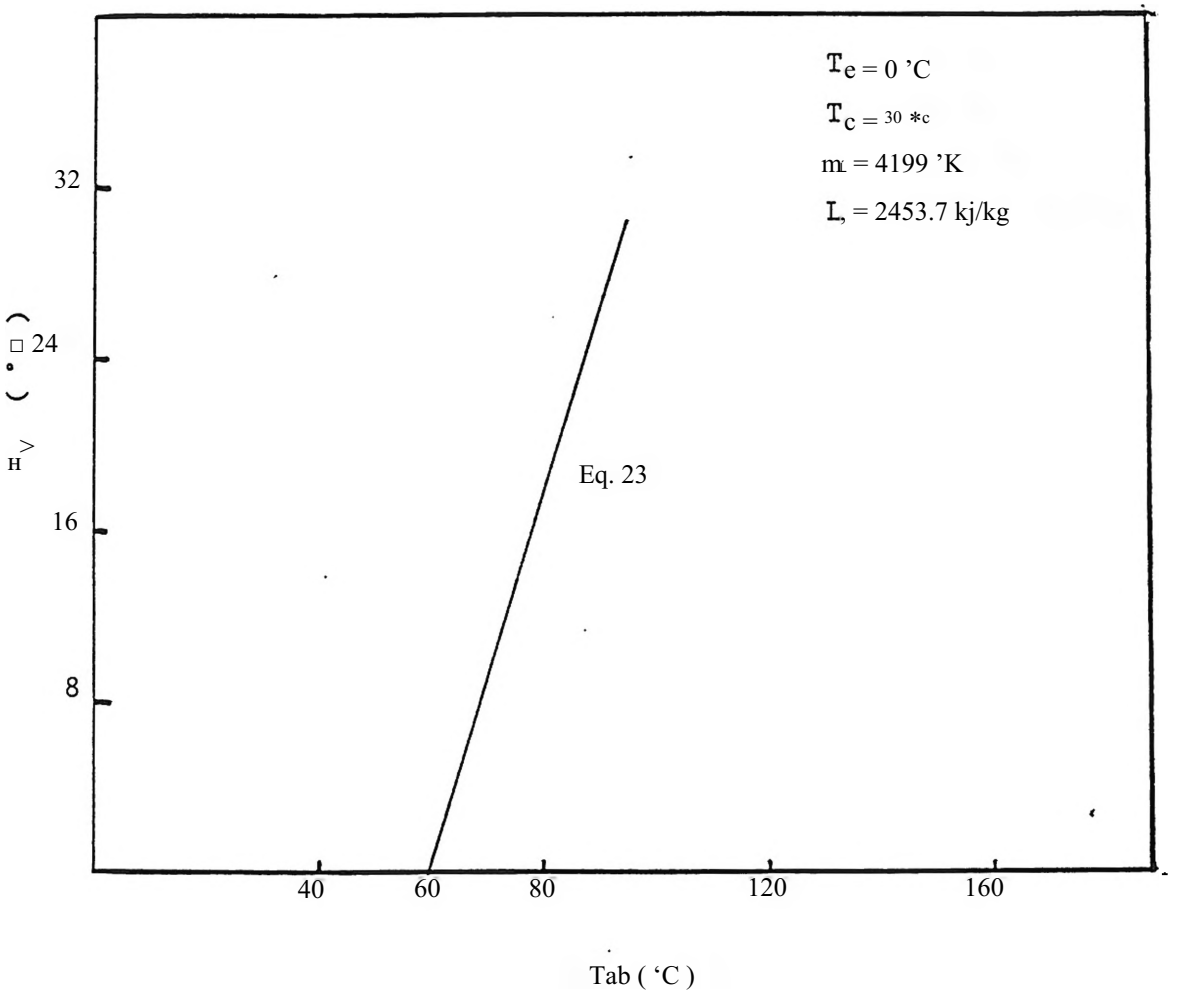

Fig.13 The Linear Relation between T_v and in the Absorption T_{ab} Properties Equation.

where m_b and C_b are constants. Using the steam tables, Ref.22, to determine the slope, m_u and C_L for water yields

$$L = -\frac{7}{3}(T_v) + 3137 \qquad (25)$$

where the units in Eq.(25) are L: (Kj/Kg), and Tv: (K).

Inserting Eq.(24) into Eq.(1?) .yields

$$\frac{d\,Py}{P_V} = (m_L \times Ty + C_L)\ \frac{d\,T_V}{R\ T_V{}^2} \qquad (26)$$

Integration of Eq.(26) (now, L is not taken as a constant) gives the Pv versus Tv relationship for the water vapor (absórbate) in the phase transformation as

$$\ln P_V = -\left(\frac{C_L}{R} \times \frac{1}{T_V}\right) + m_L \times (1/R) \times \ln T_V + C_W \qquad (27)$$

where C_w is a constant (C_w = 48.11 bar) when Tv varies, from 0 to 30 C (unit for Pv is bar). For the zeolite-water pair, Eq.(15) can be written as

$$\log P_v = -m_z(1/T_Z) + C_z \qquad (28)$$

or

$$\text{In } P_v = e^{m_z\left(\frac{-1}{T_Z}\right) + C_z e} \qquad (29)$$

where Cz is a constant for each different constant mass line (see Fig.12). Now comparing Eq.(29) and Eq.(27) gives

$$\frac{e^{\prime\prime z}}{-1_z} + \cdot eC_z - C_w - \frac{C_L}{R} \times (1/T_V) + m_L(l/R) \times \text{in } T_v \quad (30)$$

This relationship,Eq.(30), is based on the zeolite-water pair phase transformation. Using this expression one can plot the isoster of Tv versus Tz for L being a function of temperature (to be shown in Fig.14). Now Eq.(30) can be written to explicitly determine Tz as

$$T_z = \frac{-m_z e}{C_w - \frac{C}{RT_V} - JI'' \pm m_L(l/R) \times \text{In } T_v - eC_z} \quad (31)$$

Equation (31) shows the relationship between absorber and absórbate temperatures (based on the heat of vaporation being a linear function of temperature). Where Cz is a* constant on the same constant mass line (see the log Pv versus 1/Tz plot shown in Fig .12). Taking data of Tz, Pv, and mz from any point (on a i-th constant mass line) as a boundary condition of equation (29), Cz of the i-th constant mass line can be computed as

$$Czi = -\left(C_w \frac{1}{e} \frac{c_T}{RT_V} \pm m_L(l/R) \times \text{In } T_v + \frac{em}{æzi}\right) \quad (32)$$

where in this case, Tz=Tzi. Now inserting the Czi value computed from Eq.(32) into Eq.(31) the i-th constant mass line in Tv versus Tz coordinates can be obtained. The Tv versus Tz line for each i-th constant mass line is nearly a straight line as shown in Fig.14. The temperature of desorption (shown in Fig. 14) for each line is the location where the corresponding vapor condensation temperature (Tv) equals Tc. Thus the desorption temperature for the i-th constant mass line can be expressed as

$$T_{di} = \frac{-m_z e}{C_w - \frac{4T_c}{K_1 Q}(1/IO \ln T_c - C_z i(e)} \quad (33)$$

Also the absorption temperature for each i-th line is the location where the corresponding evaporator vapor temperature is Te. Therefore the absorption temperature can be expressed as;

$$T_{ai} = \frac{-em_z}{c_w - \frac{1}{K \chi e} + m_z(1/R)\ln T_e - eC_z i} \quad (34)$$

Equations (33) and (34) show the refrigerant (absórbate) desorption and absorption temperature are both related to the absorption pair properties.

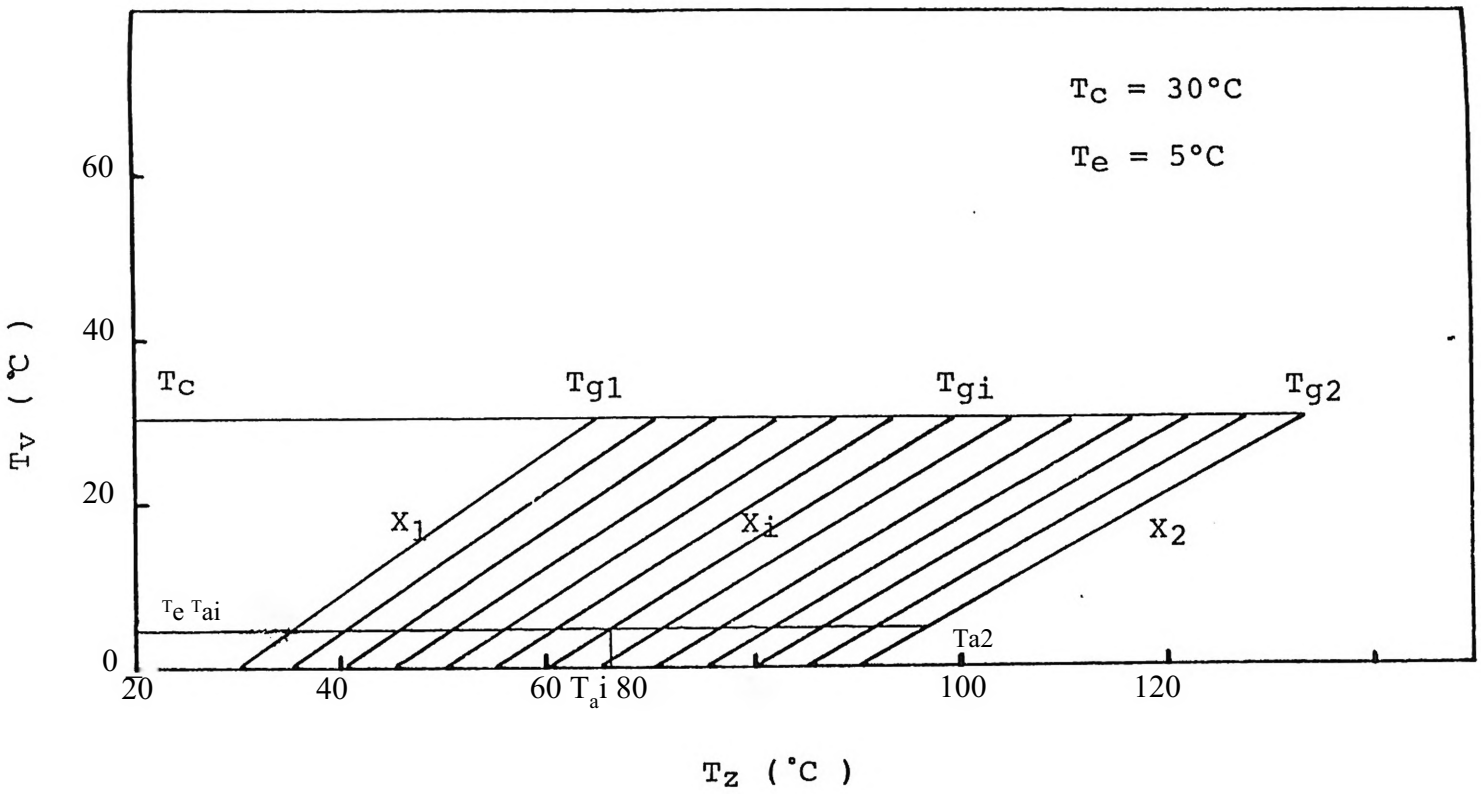

Fig. 14 T_v Versus T_ζ Plot for Zeolite (13X) - Water Pair

3.5 K^аи^зЬжР_Ll£l^^п_3£1^г_C2Ll£c£ш:_Ш^£1^су._.аш1

áhs.úEE¿ion_Erú£srLiss

There are several types of solar collectors. The main three types used for flat-plate solar collectors are (1) S-type (which is a single-glass flat-plate collector), (2) P-type (which is a double-glass, flat-plate collector), and (3) V-type (which is an evacuuated flat-plate collector). The collector efficiencies of these 3 types are nearly a linear function of collector temperature. A mathematical expression for the efficiencies of these 3 types of collectors can be expressed as

$$^{co} = {}^{m}co \times Teo + Cco \tag{35}$$

where mco and Cco are constants and depend on the type of solar collector. To simplify the analysis, the temperature both of the collector and of the zeolite in the system were assumed to be equal. This implies the heat exchanger (coupling heat transfer between the zeolite and the solar collector) efficiency is equal to unity. It should be noticed that before the zeolite reaches the initiation desorption temperature, there is no mass circulating in the refrigeration cycle, thus the CP will be zero. After reaching the desorption temperature, there is some mass

circulating in the refrigeration cycle and the system CP will increase gradually. The temperature of the zeolite will be equal to the desorption temperature of each i-th constant mass line. This means that Teo (collector temperature) = Tzi = <Tgi after the beginning of desorption. Employing Eq.(33) (Teo = Tgi) and combining with Eq.(35) yields

$$\text{^20 - mCO}^{\overline{x}} \quad (\quad \text{- ------ ČF“----- ΠΓΤΣ----T“1 + Cco} \quad (36)$$

Cw’^T+mL__S---------- eCzl -em_zi λ

Equation (36) shows that the solar collector efficiency is also affected by the absorption properties (constant sets mzi and Czi), and the solar collector type (constant mco and Cco).

3.6 Lns±ânlê2Us_ÇE_£ûr_Sûl.a _ _r_Zeolite_Refrigeration_System

t

Combining Eqs.(36), (6), and (18) gives the result

$$\text{CPai} = \text{~}_{\mu m}\text{—Γ"(----------- FT------ + Cco)'^37)} \quad t \circ \text{'y} \mid$$

eRm_zi ~*L , — θ (m 21) χ (mco) f-, \

CL , mL(ln T_c) - Cw, RT_C ---------- Ř---------- eCzl

Equation (37) shows that the instantaneous system CP is affected by: (1) the absorber properties (mzi and Czi), (2) the working temperature Tc and Te in the refrigeration cycle, and (3) the solar collector types (Ис and Cc).

Recall that the zeolite properties equation constants Czi are related to Tzi, where Tzi (the absorption temperatures) are dictated by the ambient temperatures (during the night-time cycle). Therefore the instantaneous system CP is also determined by the ambient (condenser) temperatures.

3.7 Mean CP for Zeolite Refrigeration System

The instantaneous system CP, Eq.(37) has been derived by considering the working fluid properties (on a per Ibm basis), but the amount of working fluid in the refrigeration cycle has been ignored. For the absorption system the working fluid in the refrigeration cycle comes from mass desorbed at the absorber. The instantaneous system CP means nothing without quantifying the working fluid mass. The mean system CP of the zeolite absorption system is defined as

$$CP_{mt} = \frac{\sum_{i=b}^{c} [L \times (Xi-Xi-1)]}{\sum_{i=b}^{c} [(Xi-Xi-1) \quad \frac{(¿H_{i-J} + AH^{\wedge}}{2 \times 'J_{i}}]} \qquad (3\ 8)$$

where Xb is the water mass concentration of the zeolite at the beginning of the entire desorption process. The value Xc is the water mass concentration of the zeolite at the end of of the entire desorption process. The symbol Xi is the water mass concentration of the zeolite at the i-th constant

mass line between Xb and Xc. Accounting for the sensible heats (thermal capacity) of the generator (sorbent and sorbate) will reduce the performance given by Eq.(38). Allowing for the influence of these thermal capacities in an absorption cycle abed (shown in Fig.8b) yields

$$CP_m = \frac{\sum_{i=b}^{c} V_f L \times (Xi-Xi.i)]- Qi}{\sum_{i=b}^{c} rt\ (Xi-Xi-1)\frac{(\Delta H_{\cdot} \cdot i+AHi)}{2 \times 41}\ ]+02+03} \quad (39)$$

Where Q1 is heat necessary to cool the sorbate from Tc to Te, the expression for Q1 is given by

$$Ql = \Sigma\ C \sum_{i=b}^{c} (Xi\text{"}Xi-1)(h_c\text{-}he)\ ] \quad (до)$$

Q2 is the heat necessary to bring the mass of the sorbate (1) from Tza to Tzb (Xz is constant) and (2) from Tzb to Tzc (Xz is not constant), the expression for Q2 is given by

$$Q_2 = \Sigma\ t\frac{Ъ\ ^{x}a\hat{\imath}\text{-}\ \hat{}i\text{-}l\hat{}}{i\text{-}i\text{-}\acute{c}i} \cdot \cdot \cdot \cdot \cdot \cdot \cdot l\_\pm\_\sum_{i=b} [\frac{C\ ^{*}i(hi\text{-}hi.i)}{\hat{}i} 1 \quad (41)$$

Q3 is the heat necessary to bring the mass of the sorbent from Tza to Tzc (mz is constant), the expression for Q3 is given by

$$\$3 \text{“}\text{–} \sum_{\text{Í = ČL}}^{b} S\text{Ţ}\ [\ C_{pz} \times (Tz\text{ị}\text{-}Tz\text{ị}.i) \times \frac{1}{\eta_i}\ ] \quad (42)$$

CHAPTER IV

Results and Discussion

Having developed the governing expressions for the thermodynamic behavior of the solar zeolite refrigeration system, the results will now be presented as a function of governing parameters.

4.1 ÇnoinS.rÍSén_aéÍKéén_Iyé-Méthod^_o£_f^t£rniÍnLng Réfrigérant- £пттп£1оп_1ппШПГа£цце^

The effect of L being a function of temperature can be shown via Eq.(31). The two expressions, Eq.(23) (L assumed constant) and Eq.(31) (L assumed a function of T) are plotted in Fig.15. The results in Fig.15 show that Eq.(23) predicts the desorption temperature to be slightly higher than Eq.(31). It should be noticed that applying the boundary condition of the absorption refrigeration cycle (where as Tv=Tc,then Tab=Tg, and as Tv=Te, then Tab=Ta) to Eq.(23) yields

$$L\left(\frac{1}{T_e}-\frac{1}{T_c}\right)=a_H^1\left(\frac{\cdot}{}-\cdot\cdot\frac{1}{T_a}\,\frac{1}{Tg}\right) \qquad (43)$$

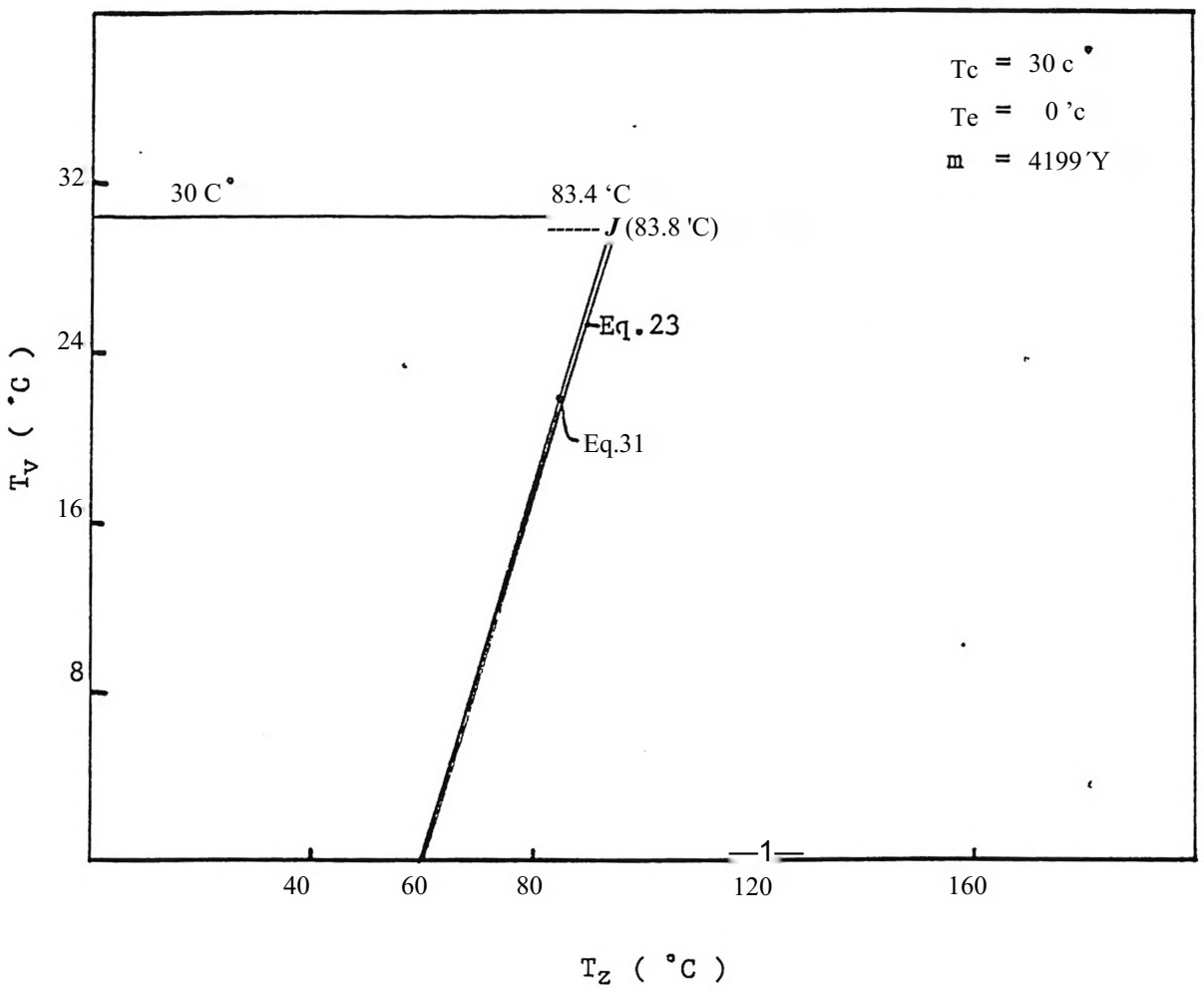

Fig.15 Comparison between Eq.31 (L depend on T) and Eq.23 (Constant L).

Equation (43) is the same as Eq.(7). Since Eq.(7) has been checked with experimental data by Ref. 10, this implys that Eq.(31) and Eq.(23) are correct. However Eq.(7) only shows relationships between ΔH and two special points (desorption and absorption points). Equation (23) shows the relationship between absorption properties and any point on the line of Fig.15. Equation (31) agrees well with Eq.(23) except the applicable temperature range of Eq.(31) is wider than Eq.(23). Since (1) the relationship between desorption temperature and slope, m and (2) the relationship between heat of absorption,ΔH and slope, m have been found (Eq.(23), Eq.(31), and Eq.(14)), therefore the system performance for various types of zeolite can be predicted by varying the slope, m (unlike Ref.10 where evaluating all types of zeolite ΔH was required experimentally).

4.2 E££e£t_û£_Ahs_Qrbs.r_Sloa^on tliÊ 2ê£ri^rant. Desorption_Temperature

Since high temperatures yield low solar collector efficiences, low desorption temperatures are desirable for solar refrigeration. The refrigerant desorption temperature is related to the absorption properties as shown in Eq.(33). These absorption properties depend on the absorption pair and can be represented by the constant mass lines on a log-

Pv versus 1/Tz plot. One of the main paramaters for the constant mass lines is the slope, m. In order to see how the refrigerant desorption initiation temperature will be affected by a different absorption pair, Eq.(33) has been employed by holding all parameters constant except slope, m. The results are shown in Fig.16; here it is seen that higher m values result in lower desorption temperatures. Therefore the desorption initiation temperatures for three different absorption pairs which start at the same point, Ta, (as represented by Ref.10 in Fig.5) does not agree with Eq.(33). This can result in significantly different performance curves than show in Fig.5.

4.3 Relationship Between System CP and Generator Temperature

The dependence of the system CP as a function of generator temperature is shown by the five curves (A,B,C,D,and E) in Fig.17. Curve A represents the Carnot cycle efficiency, (Eq.2); curve B represents the Carnot cycle efficiency based on the absorption working temperature, (Eq.3). Curve C represents the absorption cycle efficiency, (Eq.8); curve D represents the mean absorption cycle efficiency, (Eq.39), assuming a solar collector efficiency of unity. Curve E represents the mean absorption cycle efficiency (Eq.39) based on a solar collector efficiency which is a function of

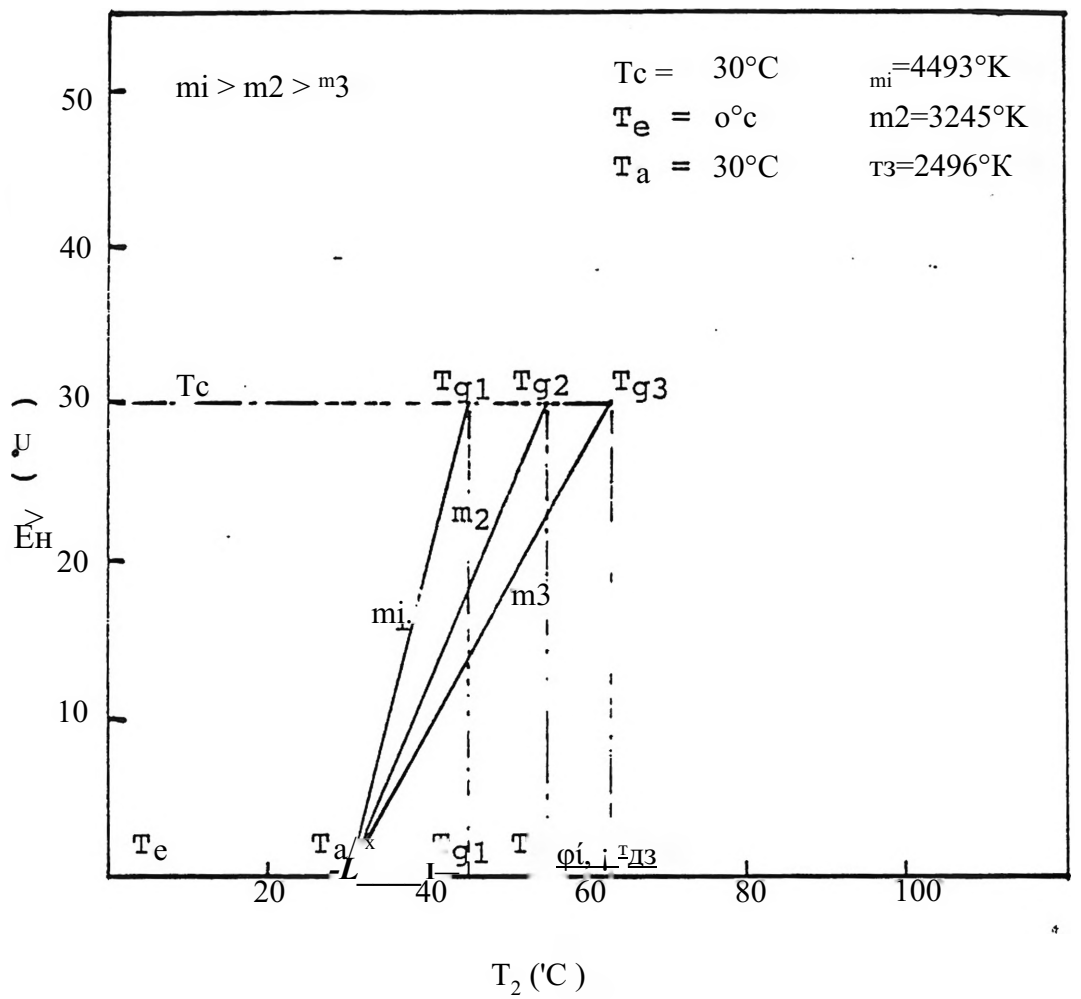

Fig. 16 Effect of.the Slope, m, on Desorption Temperature based on Eg. (33).

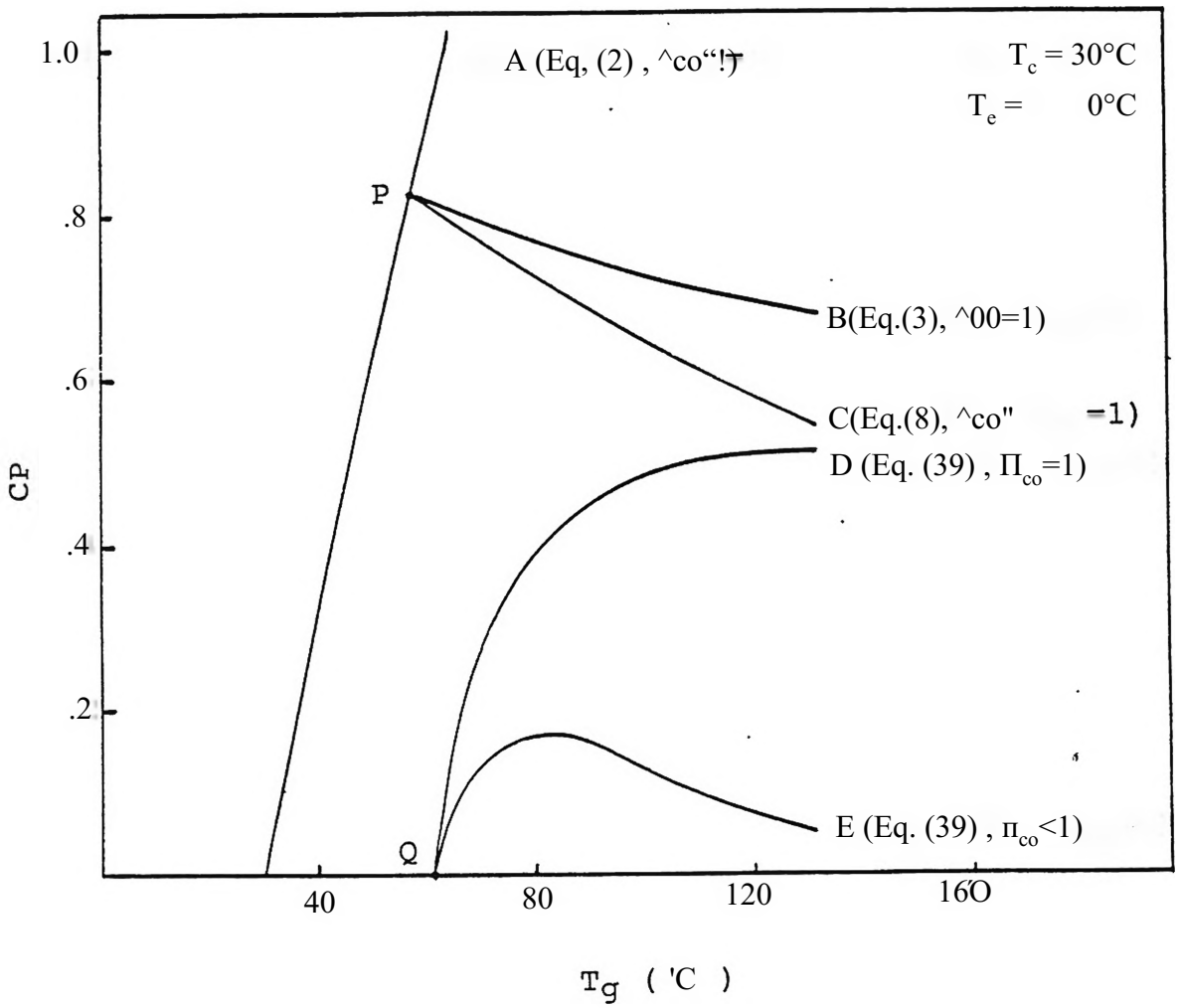

Fig. 17 System CP Versus Generator Temperature.

temperature. It should be noted that before reaching the initiation desorption temperature there is no working fluid mass in the refrigeration cycle. Since there is no mass flow before reaching the intiation desorption temperature, curves D and E in Fig.17 are zero until reaching point Q ($T_a=T_w$), where point Q is the intiation desorption point. Points P and Q are the same initiation desorption temperature. The mean CP (curve D) increases sharply when Tg increases beyond point Q, however as Tg increase the instantaneous CP (curve B) eventually begins to decrease; this causes the mean value (curve D) to decrease. Therefore a maximum mean CP is achieved after Tg increases beyond point Q on curve D. Since the solar collector efficiency also decreases as Tg increases, the system overall mean CP (curve E) will decrease more rapidly than curve D. Curve E represents the limiting overall mean CP for the case of curve B.

4.4 The Optimum Uniform Slope

The zeolite absorption refrigeration system overall CP is affected by the slopes (of the constant mass lines in Fig.12). For most zeolites these slopes slightly increase as their mass concentration X decreases. To simplify the Problem it was assumed that each zeolite had a constant slope (mz) for all the various constant mass lines. By

varying this uniform slope, which implies changing the zeolite type, the system overall mean CP as a function of slope (mz) was computed from Eq.(39) and is shown in Fig. 18.

From Fig. 18b it is seen that the mean CP is a strong function of slope (mz) for the V-type flat-plate solar collector, while the mean CP is- a weak function of mz for the P-type flat-plate solar collector. A maximium mean CP occurs for each type of solar collector (V,S,P). The optimum slope, mz value, is defined as the ideal slope. The ideal slopes decrease as the solar collector efficiency increases. The ideal slope for a V-type collector occures at point a. This mz value is lower than typically occurs in natural zeolites, thus there is some possibility that a better absorption pair may be available for the intermittent absorption refrigeration system for this type collector.

4.5 Lff£oI^o£_N^i-Unif_ôĽm_l£QXi.te_Sl£pe._

in the above section (4.4) it was assumed that the slopes, mz, were uniform to find the optimum value of the uniform slope. In this section computations were preformed for a zeolite with non-uniform slopes. To show this effect the set of slopes for the zeolite(13X)-water (Ref.20) was chosen. Then by varying each constant mass line slope by a

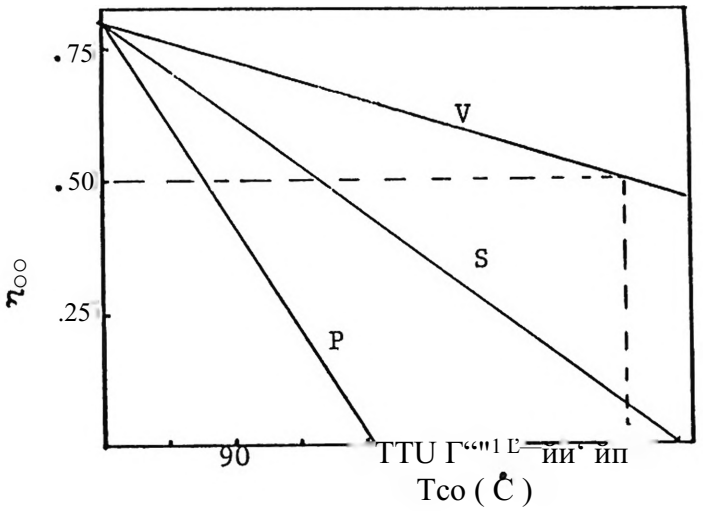

(a) Solar Collector Performance

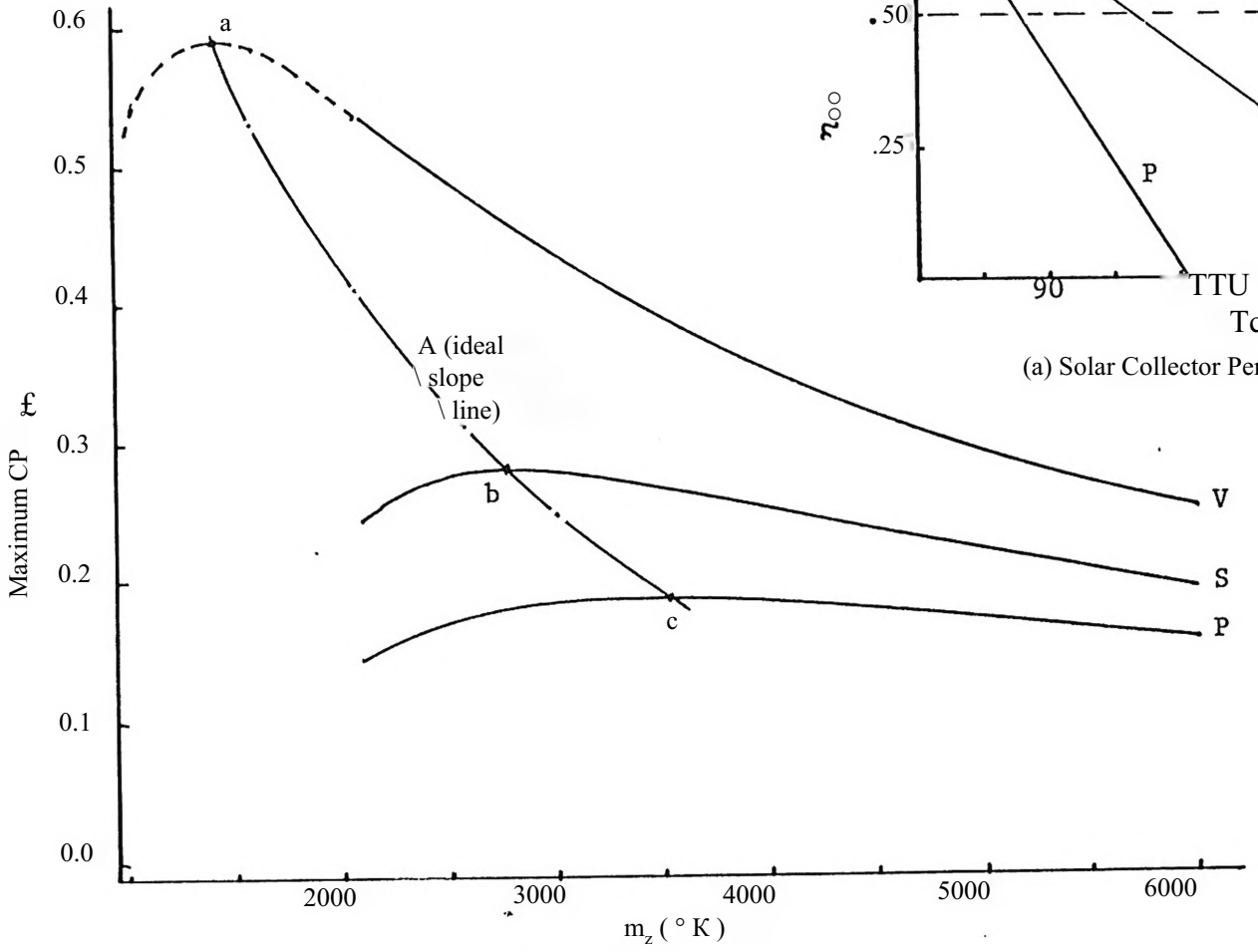

(b) CP Versus m_z

Fig. 18 Idealizied Slope at Tc=Too = 30 °C, T_e = 0 C.

constant factor, a' simulation of various types of zeolite-water pairs was achieved. In order to show how the system CP was affected by the non-uniform slopes of the zeolite mass absorption properties, Eq.(39) was used for the zeolite(13X)-water pair to compute mean CP values. The results are shown in Fig. 19 where the solar collector performances are shown in Fig.18a. In Fig.19 there are three curves, A, B, and C. They are generated by assuming Xz = 0.280-0. 1 90, and Cpz = 0.963 (kj/kg, K). Curve C (m = 2500-3000) is the standard zeolite(13X)-water pair and represents the lower-slope type of zeolite-water pairs. Curve B (m = 3250-3900) represents the result of the middle-slope type of zeolite-water pairs. and curve A (m = 4500-5400) represents the high-slope type. As seen curves A, B, C in Fig.19 each have a different initiation desorption temperature. The lower-slope-type always has the highest initiation desorption temperature. Also the maximum CP is quite different for curves A, B, C, (Fig.19) which corresponds to the V-type solar collector. These maximium CP differences are insignificant corresponds to the P-type solar collector.

The starting points on curves A, B, C (in Fig.19) are the initiation desorption points. These separate initiation desorption points on curves A, B, C shown can be deduced

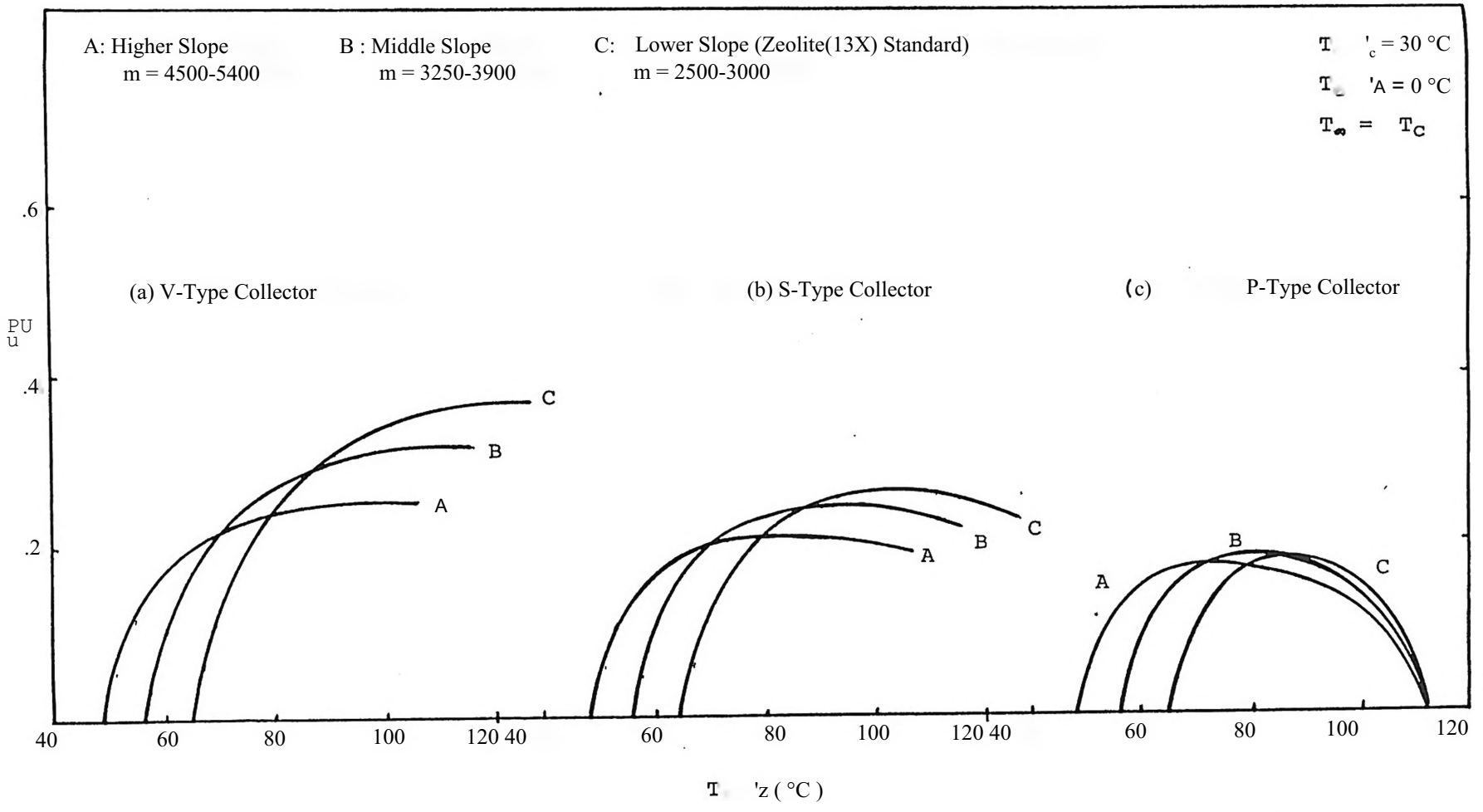

Fig.19 Effect of Non-Uniform Zeolite Slope

cn
(JI

from Eq. (33) and agree with Fig. 16. A low initiation desorption temperature allows the solar collector to operate at a lower temperature range but has a higher slope (mz) value which implies having a higher heat absorption value (see Eq.(14)). Therefore the slope, mz, has competing effects. (1) The higher slope helps the system CP by operating at lower generator temperatures and hence higher solar efficiencies. (2) The higher slope has higher heat absorption values which lowers the refrigeration cycle COPr value (see Eq.6)). Hence there are two coupled effects governing the system overall mean CP as a function of the slope, mz. Due to these two combined effects the results in Fig.19 become understandable. (1) For a system using an evacuated solar collector, the collector efficiency is a weak function of temperature*(with respect to collector working temperature) and hence is not strongly affected by the desorption initiation temperature. Therefore the mean CP is primarily influenced by the second effect (i.e. from the low mz value yielding a low heat of absorption value) which causes a higher overall mean CP to be achieved by the lower mz (curve C). (2) For the system using a P-type solar collector, the collector efficiency will drop sharply as the working temperature increases, thus both the effects of varying the slope, mz, are competing in such a manner that Fig.19c indi-

cates only a weak influence on the maximum overall mean CP for the three different curves A, B, and C.

In summary, the heat of absorption value is not important to the zeolite absorption refrigeration system maximum performance if a simple P-type flat-plate solar collector was used.

4.6 Effect of Ambient Temperature

The ambient temperature is the limiting temperature for heat rejection. During the absorption process a lower temperature for heat rejection will produce a higher water mass concentration in the absorber. This in turn lowers the desorption initiation temperature. Therefore the solar collector can work at lower temperatures, and hence improve the overall mean CP. By holding all parameters constant except the ambient temperature, the ideal slope (see $_s$ Fig.18b) can again be determined; these results are shown in Fig.20. It can be seen that the ideal slope values increase as the ambient temperature increases. Line G in Fig.20 shows the optimum zeolite slope at an ambient temperature of 30 C for three types of solar collectors, where the ideal mz values (points 1,2,3) correspond to points a,b,c in Fig.1 8b. The system mean CP is also dependent upon the ambient temperature as mentioned before. By varying the non-uniform

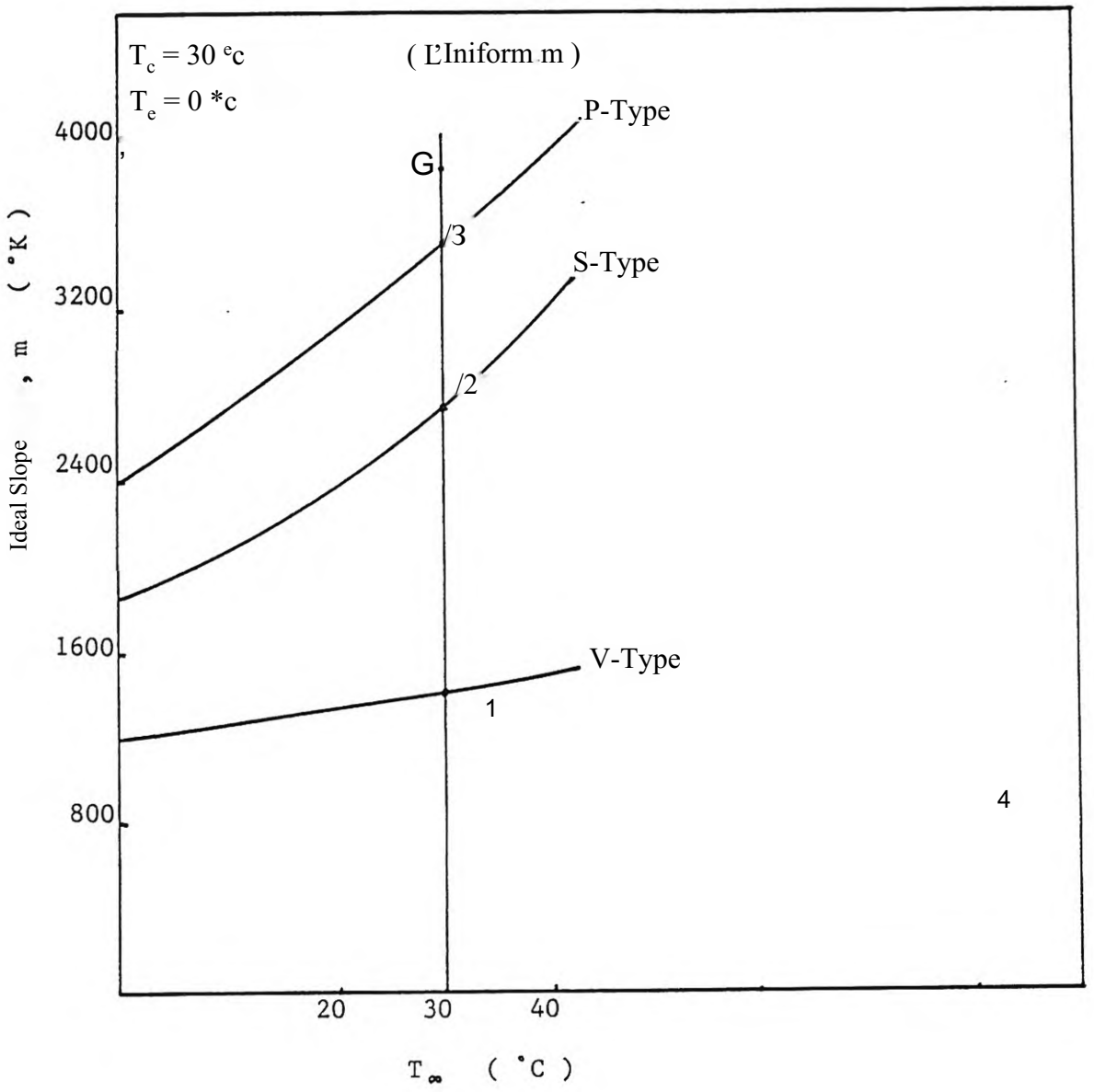

Fig.20 Ideal Slope as a Function of Ambient Temperature.

slopes (the three zeolite-water pairs having non-uniform slopes are generated in the Section 4.5) and holding all parameters constant except the ambient temperature, the mean CP dependence can be determined. The relationship between mean CP and ambient temperature is presented in Figs.(21,22,23). These figures correspond to the P-type,S-type, and V-type solar, collectors respectively. At the typical ambient temperature of 30 C the peak mean CP has been indicated by points 1,2,3 on line G (in Figs.(21, 22,23)), these points agree with points 1,2,3 in Fig.19. Since the lines (A,B,C) in Fig.21 cross each other, this implies that the zeolite type should be selected according to the collector type and the ambient temperature expected at a particular geographical location.

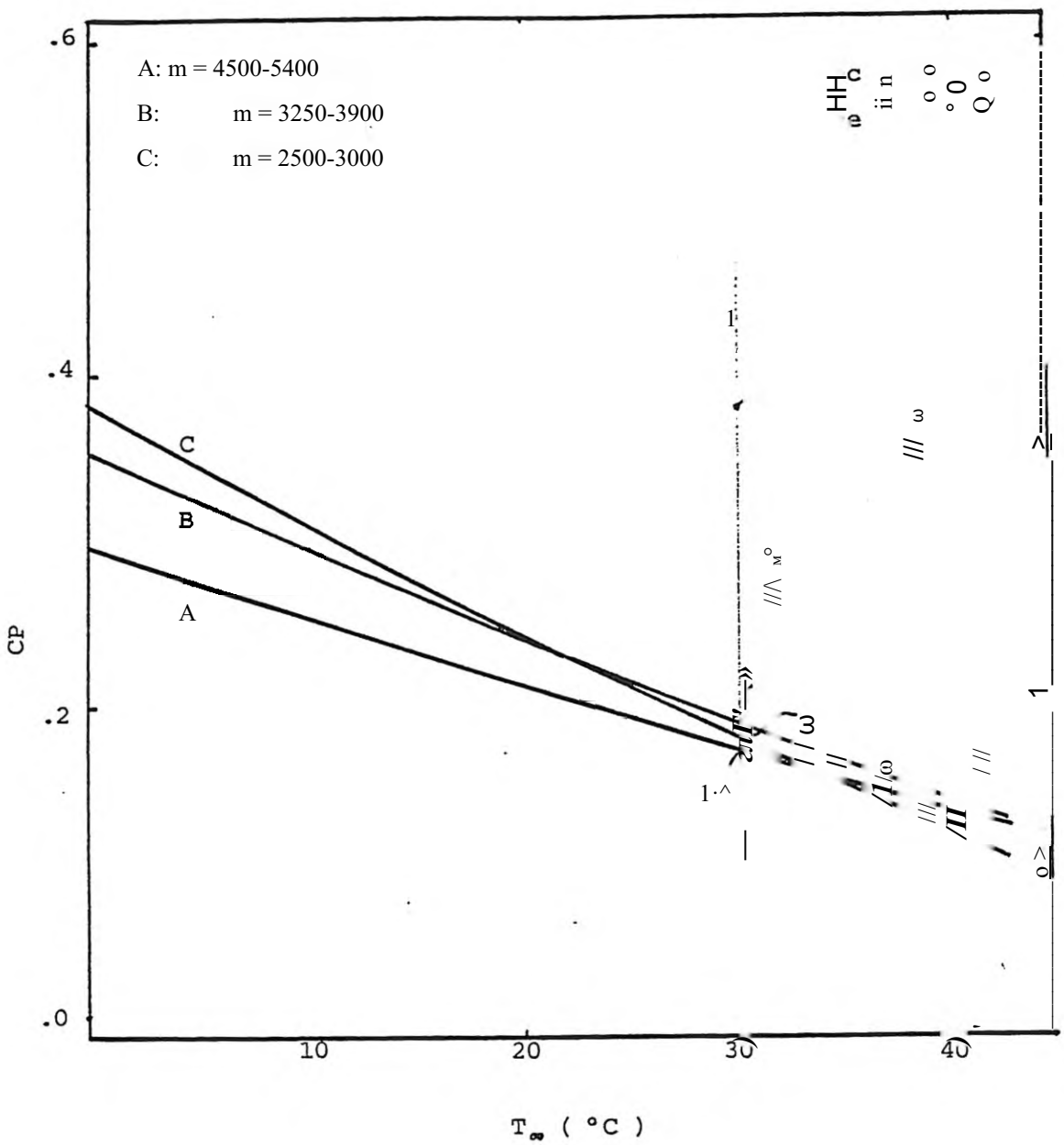

Fig.21 Effect of Ambient Temperature on CP for P-Type Collector.

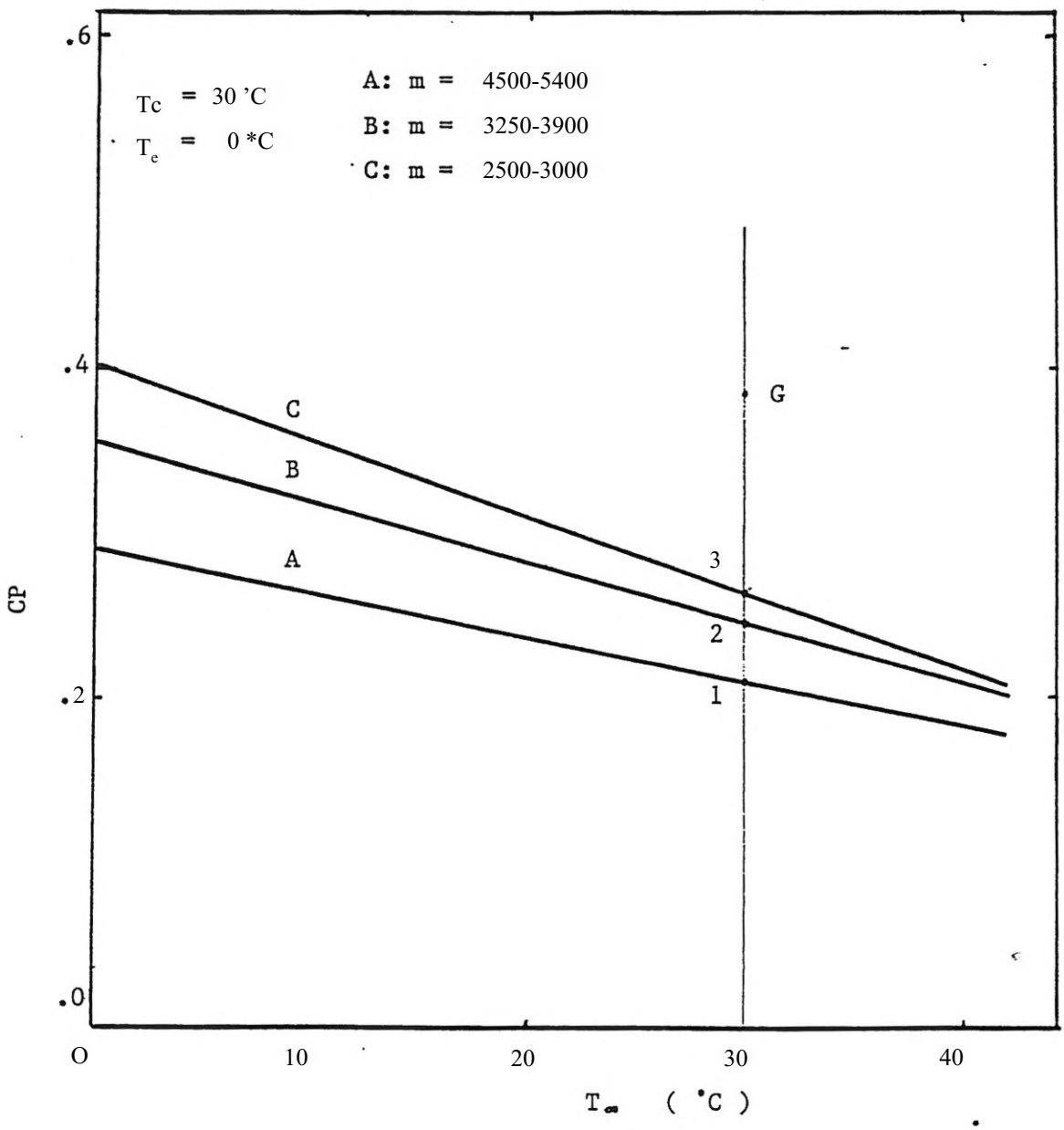

Fig.22 Effect of Ambient Temperature on CP for S-Type Collector

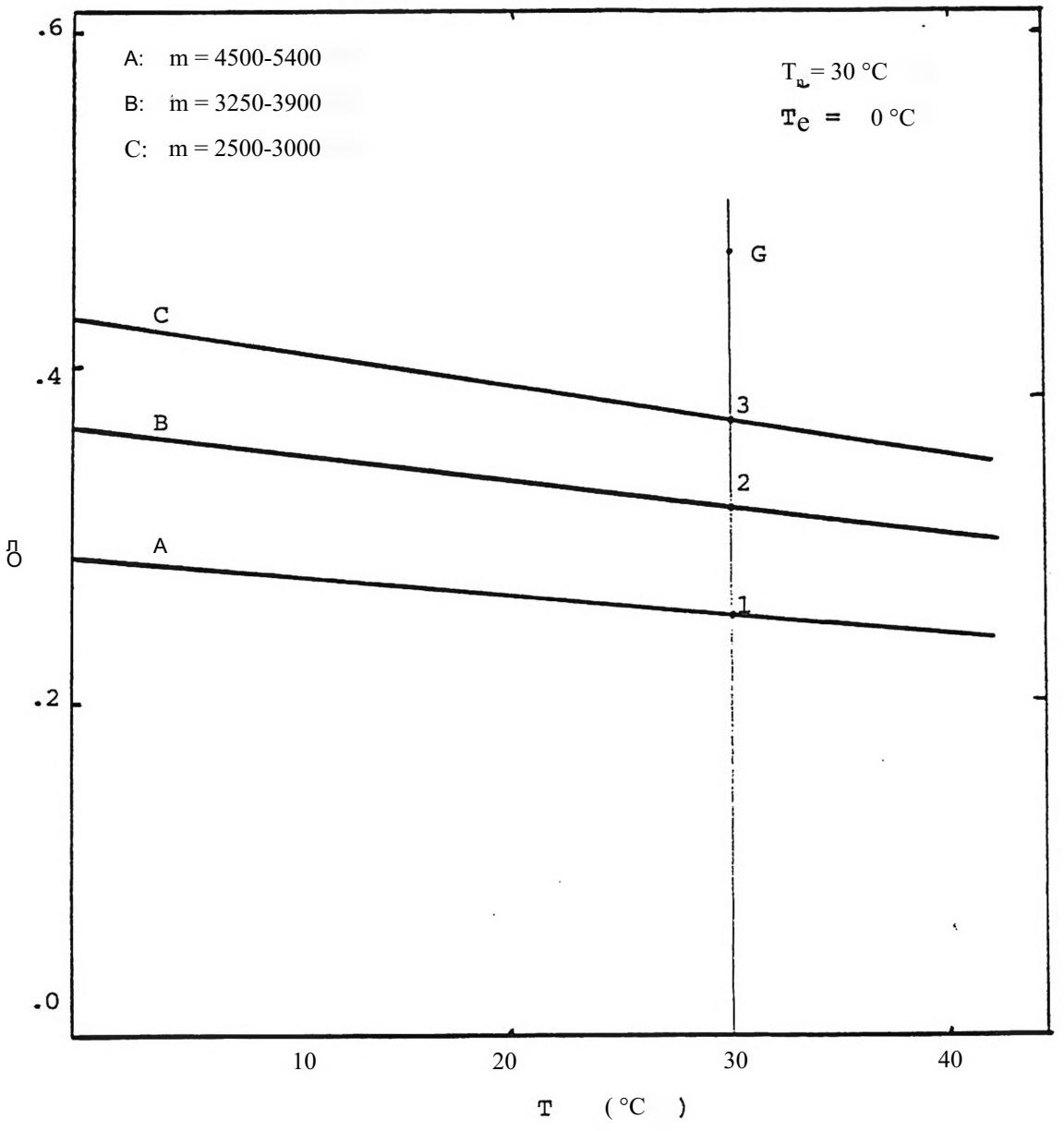

Fig.23 Effect of Ambient Temperature on CP for V-Type Collector.

4.7 Cornpa ri son-B^tw^^P-the ■Z.g.o.lit _e(13X)-Water lntérnii¿tént_and—LiBrdiai^-CúrLLíimúu^í^ :le

Using the slope, m to find the desorption temperature, the continuous absorption refrigeration system CP also can be determined. A comparison between the zeolite(13X)-water intermittent cycle and the LiBr-water continuous cycle is presented in Fig.24.

The curves A,B,C (Fig.24) are the same as in Fig.19 (P-type collector generated by three different slope types) and represent the Zeolite(13X)-water intermittent cycle performance. Curve D was generated by the LiBr-water system under the same operating condition (indicated in Fig.24) as curves A,B,C and represents the LiBr-water continuous cycle performance. As seen the LiBr-water m value is lower than that of the zeolite-water, which causes a low value of heat of absorption and a high value of the desorption temperature (79-36°c or 174-1 87 *F). It is true that the low heat of absorption value will produce a high COP for the LiBr-water absorption refrigeration system (without using a solar collector). However the high desorption initiation temperature increases the working temperature range of the solar collector. It should be noticed that system performance is decreased sharply by the low collector efficiency.

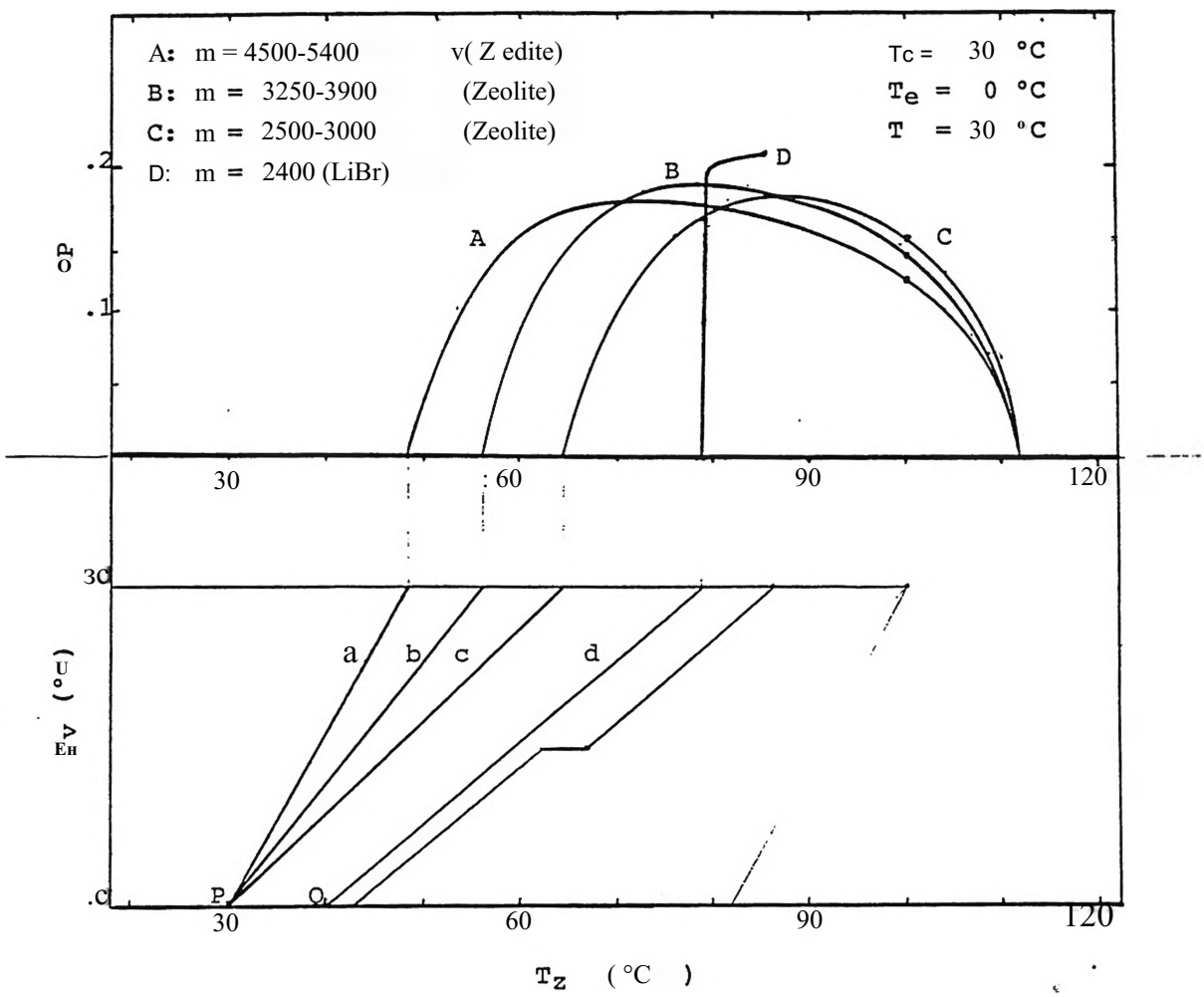

Fig 24 Comparison between Zeolite-Water Intermittent and LiBr-Water Continuous Cycles for a P-Type Collector.

Moreover the temperature difference between day-time and night-time operation in Mississippi is about 10'C, Ref. 23. Thus there is about 10 °C heat rejection-temperature difference between the LiBr-water continuous system (heat rejected during day-time) and the zeolite-water intermittent system (heat rejected during night-time). Due to this 10 C temperature difference, the absorption initiation point P of line a,b,c is different from that (point Q) of line d as indicated in Fig.24. Based on the LiBr-water desorption temperature range (79- 86 * 0), the solar collector efficiency for the P-type collector operating at 86 °C (the continuous type solar collector working temperature must be higher than the peak temperature of the desorption temperature range) is only about 0.288. However the LiBr-water system COP (without using a solar collector) is about 0.75 (Ref.10). But when this value is multiplied by the collector efficiency, the system overall mean CP becomes 0.216. Comparing both systems (Fig.24) the system overall CP for the LiBr-water shows a slightly higher value than the zeolite-water system for using P-Type solar collector. Comparing for using S-Type and V-Type solar collector has shown in Fig.25.

The heat rejection-temperature (heat absorption) range of the LiBr-water system is very narrow (40-47 °C shown in Fig.24). This is because of the crystallization limitation

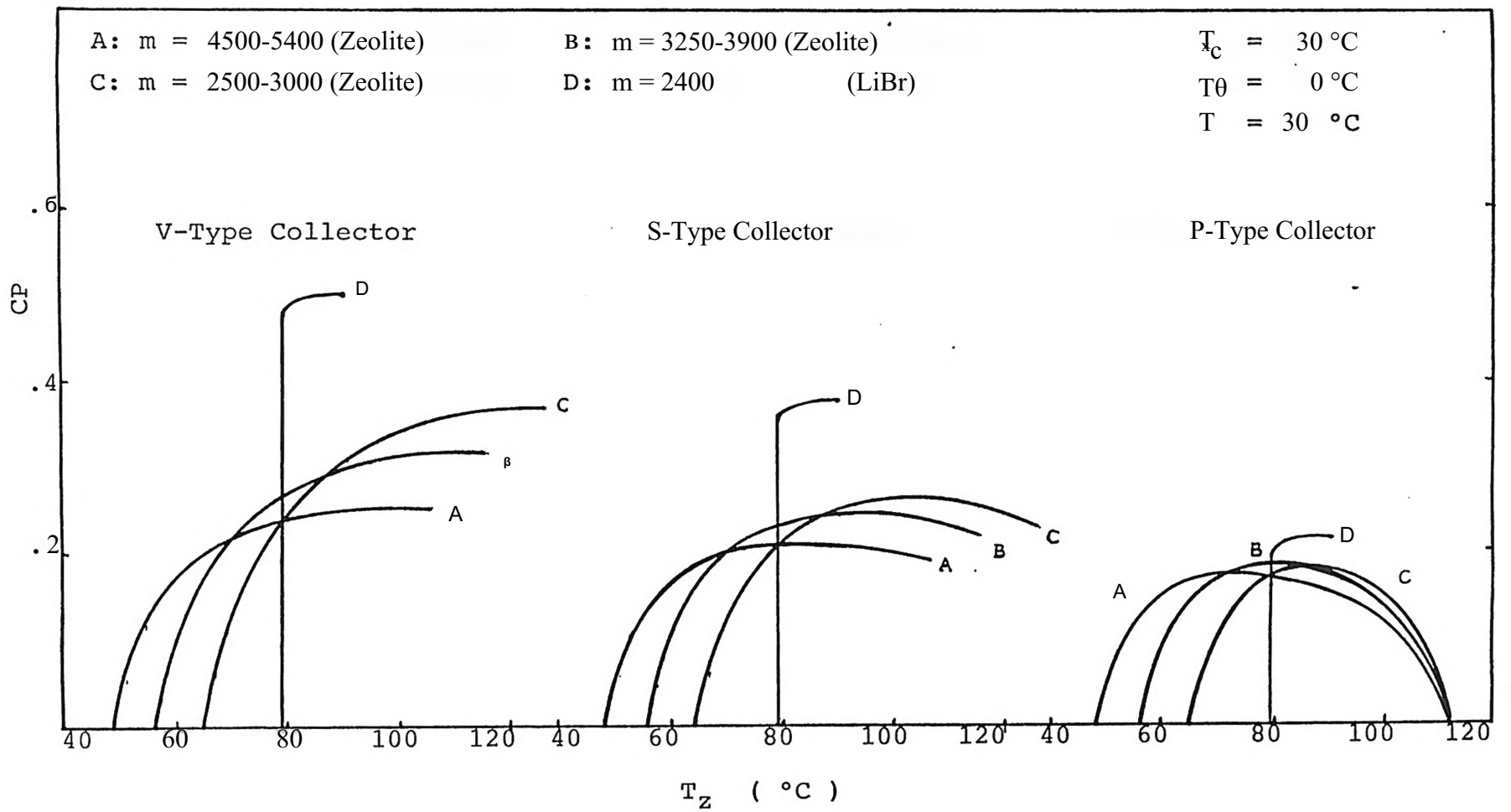

Fig.25 Comparison between'Zeolite-Water Intermittent and LiBr-Water Continuous Cycles

which occurs for the LiBr-water absorption pair. Due to this limited heat rejection temperature range, production of hot water as a by-product is difficult to achieve. Also the LiBr-water pair requires the rejection of large amounts of heat. This will be difficult to achieve on a hot summer day and hence a water cooling system will be required for the LiBr-water continuous absorption refrigeration system.

On the other hand, the zeolite-water intermittent cycle has a overall mean CP slightly less than the LiBr-water system (see Fig.24 line A,B,C and D) for the P-type solar collector. However the heat rejection temperature range for line A (30-80 'C) is much wider than line D (40-47 *C); this range is useful for producing domestic hot water. Due to the wider range of heat rejection temperatures, and since the heat rejection time is at night, thus a longer time period is available and a lower ambient temperature is , available for rejecting heat. Hence water cooling equipment is not necessary for the zeolite-water intermittent cycle.

As seen in Fig.24, the narrow working temperature range for the LiBr-water system (heat desorption at 79-86 °C, heat rejection at 40-47 °C) will cause the system to stop functioning: (1) during bad weather, the solar collector cannot provide heat in the temperature range 79-86 C, and (2) on

hot days when the ambient temperature is higher than 40 °C during the day-time. The zeolite-water system can operate during most days because of the wider working temperature range as shown in Fig.24.

4.8 System Cost and Sizing

In order to estimate the cost and size of a zeolite(13X) refigeration system, the cooling load for a typical house was computed as shown in Table II. The energy input for the air-conditioning of a typical family dwelling of approximately 2000 ft^2 of living space was assumed as shown in column 2 of Table III. Based on C0Pr=2.0, the cooling load was computed (column 3).

The total zeolite mass of a zeolite refrigerator system is a function of the cooling load per unit mass of zeolite. Table III shows the zeolite mass required to cool a typical 2000 ft^2 home (Table II). According to Table III, the total zeolite mass required is 882 kg (1940 lbm or about 4.0 fifty-five gallon drums), where $fz = 1040$ (kg/m^3). The cost of this amount of zeolite will be about $291 (based on a natural Mississippi zeolite unit price of $ 0.15/lbm).

Table II Cooling Load for a Typical 2000 ft^ House

	Power Input * (kw/Mon.)	Cooling Load ** (Power Input x COP) (kj/day)
June	300	3000 x 24
July	500	5000 x 24
August	700	7000 x 24

* Power Input to Air-Conditioner

** COP 2.0 for Central Air-Conditioning

Table III Zeolite Mass Corresponding to the Cooling

■ Load of Table II

	Cooling Load Based on kj Table II day	Cooling Effect L* x (Xc-Xb)** ' (kj/kg)	Mass of Zeolite (kg)
June	3000 x 24	190.4 kj/kg	378 kg
July	5000 x 24	190.4 kj/kg	630 kg
August	7000 x 24	190.4 kj/kg	882 kg

* Water Vapor L = 2453.7 kj/kg

** According to Zeolite(13X)-Water Pair (X_c-Xь) = 0.282 - 0.2044 (kg_w / kg_z), where X_c and Xb are Corresponding to ^21? 3>nd 2c. *

Tables IV, V, and VI (based on P-type, S-type, V-type respectively) show the solar collector area required to achieve the cooling load in Table II. The required amount of total daily-incident solar energy is a function the cooling load and the system mean performance, CPm (column 3). As Tz increases both the mass of desorbed water and CPm increase which reduces the required zeolite mass and the required amount of total daily-incident solar energy. As Tz becomes greater than the temperature corresponding to the maximum CPm then further increases in Tz will reduce the required zeolite mass but increase the required amount of total daily-incident solar energy (especially for the S-type collector). In order to reduce the required mass of zeolite, the CPm was selected at Tz = 100°C for a system using either a P-type or S-type solar collector (column 3 in Tables IV and V) and 120 *C for the V-type solar collector (column 3 in Table VI). The results show the solar collector area to be a weak function of m when using a S-type solar collector. Using a high efficiency (V-type) solar-collector can reduce (the peak value of CPm occurs at a higher Tz) the collector area and zeolite mass requirements (Table VI). The P-type collector area required is about 677 ft^2 which is about one-third the living area of 2000 ft^a ; this would require about one-third the roof area being used for solar collection.

Table IV P-Type Solar Refrigeration Collector Area Required for August

m \	Cooling Load for August Based on Table II (kj/day)	CP_m at T_z = 100 °C (Fig.l9C)	Collector Load $\frac{\text{Cooling Load}}{CP_m^{TM}}$ (B.T.U./day)	Local Solar Flux Based on Ref. 23 $\left(\frac{BTU}{day}\right)$	Required Collector Area $\frac{Load_{C}oii_{a}}{\text{Solar Flux}}$
A	7000 x 24	0.119	1340000	1972	677 ft^2
B	7000 x 24	0.136	1170000	1972 -	593 ft^2
C	7000 x 24	0.154	1040000	1972	525 ft^2

CO
H

Table V S-Type Solar Refrigeration Collector Area Required for August

m \	Cooling Load for August Based on Table II (kj/day)	CP_m at T_z = 100 'C (Fig.19b)	Collector Load $\frac{\text{Cooling Load}}{CP_m}$ (B.T.U./day)	Local Solar Flux Based on Ref. 23 (B.T.U./day)	Required Collector Area $\frac{Load_{co}}{\text{Solar Flux}}$
A	7000 x 24	0.192	828000	1972	420 ft^2
B	7000 x 24	0.223	714000	1972	362 ft^2
C	7000 x 24	0.246	647000	1972	328 ft^2

Table VI V-Type Solar Refrigeration Collector Area Required for August.

m \	Cooling Load for August Based on Table II (kj/day)	CP_m at T_2 = 120 'C (Fig.19a)	Collector Load $\frac{\text{Cooling Load}}{CP_m}$ (B.T.U./day)	Local Solar Flux Based on Ref. 23 (B.T.U./day)	Required Collector Area $\frac{Load_{co}}{\text{Solar Flux}}$
A	7000 x 24	0.254	627000	1972	318 ft^2
B	7000 x 24	0.323	493000	1972	250 ft^2
C	7000 x 24	0.369	, 431000	1972	219 ft^2

CHAPTER V

Conclusions

Solar energy is a free but low-grade energy source, therefore the system cost for applying solar energy is not always economically realistic. Applying a solar powered zeolite refrigeration system appears to be reasonable and is competitive with presently available solar energy refrigerators such as a LiBr-water system. Presently the LiBr-water system needs to use an expensive water cooling system. The zeolite solar refrigeration system can use air cooling and natural zeolite to produce cooling. The system performance was found to depend primarity upon the solar-collector type and the zeolite absorption properties. These absorption properties depend on the absorption pair and can be represented by the constant mass lines on a log Pv versus 1/Tz plot. The paramaters for the constant mass lines are slope, m, spacing constant, Cz, and water mass concentration, X.

As a result of this study some general conclusions are:

(1) The slope, m, was found to be the only variable for determining the heat absorption value, ΔH. A line of

constant mass absorption will also be a line of constant heat absorption.

(2) The slope, mz, has competing effects on the system performance. (a) The higher slope (lower desorption temperature) helps the system performance by operating at lower generator temperatures and hence higher solar collector efficiencies. (b) The higher slope (higher H value) lowers the refrigeration cycle COP and hence lowers the overall efficiency. Therefore a higher CPm will be achieved by a lower mz value when using a P-type collector and by a higher mz value when using a V-type collector.

(3) The desorption temperature predicted from assuming L to be independent of temperature agrees well with that computed by using L as a function of Tz (within the temperature range from 0-30 °C).

í²!) The instantaneous solar CP is affected by: (a) the absorber properties (mzi and Czi), (b) the working temperature Tc and Te in the refrigeration cycle, (c) the solar collector type, and (d) the ambient temperature .

(5) The optimum slope (uniform mz values) was defined as the ideal slope. The ideal slope is a function of solar collector type, and was found to decrease as the solar collector efficiency increases.

(6) In the summer time (ambient temperature assumed 30 'C), the CPm at 100'C will be around 0.12-0.15 for the P-type solar collector, it will be 0.19-0.24 when using a S-type solar collector, and 0.25-0.37 when using a V-type solar collector at Tg = 120'C.

(7) The LiBr-water continuous system was found to have slightly better performance than the zeolite-water intermittent system. However the LiBr-water continuous cycle shows a narrow heat rejection temperature range, thus a water cooling system would be required and the production of domestic hot water (as a by-product) would be difficult to achieve.

(8) The zeolite intermittent cycle had a slightly lower system performance than the LiBr-water system but had a wider operating range of heat absorption and desorption temperatures. Hence water cooling equipment would not necessary, and domestic hot water could be obtained from the heat of absorption.

(9) The water mass concentration, Xi, and the line spacing, Cz, were found to have a weak influence on the system performance but to be strong factors in determining the required mass of zeolite.

(10) The zeolite mass and solar collector (P-Type) area would be approximately 1940 lb and 677 ft respective-

ly for air-conditioning a typical house (2000 ft*)

during the summer time in Mississippi.

REFERENCES

1. Kreith, F., and Bezdek, J. F., "Can Industry Afford Solar Energy?" M^hânLçal—Eûgin^ring^ 1 976, pp. 35-41.

2. Eastop, T. D., and McConkey, A., Applied Thermodynamics fan-^Kinaering-Iaahnal·^^ London, New York, Longman, 1 97 8.

3. Prigmore, D. , and Barber, R., "Cooling with the Sun's Heat" Solar Energy-.. 1975, VOL. 17, pp. 1 85-192.

4. Reynolds, W. C., Thermodynamics, Stanford University, 1 972.

5. Epstein, M., Grolmes, M., Davidson, K., and Kosar, D., "Advanced Desiccant Dehumidification/Cooling Technology", AaME_5ih_AmiuaL_l££hnLçaL_Ç£n£ârÊn^^ 1 983.

6. Johannsen, A., "Design and Operation of a Liquid-Desiccant Type Solar Air Conditioning System", SUN II, 1979, Vol. 1, pp. 6 81-1 85.

7. Jurinak, J. J., Mitchell, J. W., and Beckman, W. A., "Open Cycle Desiccant Air Conditioning as an Alternatie to Vapor Compression Cooling in Residential Applications", ASME_Lth_AnnuaL_IêçhriiçaL_Çon£aL.ençê.4- 1 9 83 .

8. Venkatesh, A., Sriramulu, V., and Gupta, M. C., "Theoretical and Experimental Investigation of an Intermittent Solar Refrigerator", Sun II, 1979, Vol 1, pp. 749-753.

9. Tchernev, D., I., "Solar Energy Application of Natural Zeolites", NáturaL_Z^QllLé_and_I£s_U¿g.^ Oxford, New York, Pergamon Press, 1 97 8. pp. 479-484.

10. Meunier, F. , and Mischler, B., "Solar Cooling through Cycles Using Microporous Solid Adsobrents", SUN_II. Vol.1, 1979, PP. 676-680.

11. Meunier, F. , Mischler, B. , Guilleminot, J. J., and Simonot, "On the Use of a Zeolithe 13X-H2O Intermittent Cycle for the Application to Solar Climatization of Buildings", Vol. 1, 1979, pp. 739-743.

12. Alizadeh, S. , Bahar, F. , and Geoola, F., "Design and Optimisation of an Absorption Refrigeration System

Operated by Solar Energy", Vol. 22, 1979, pp. 149-154.

13. Stoecker, W. F. , and Reed, L. D., "Effect of Operating Temperatures on the Coefficient of Performance of Aqua-Ammonia Refrigerating Systems", ASH RAE. Part 1, 1971, PP. 163-170.

14. Bessler, W. F., and Chen, C. N., "Study on Parameter Variations for Solar Powered Lithium Bromide Asorption Cooling", S£Lâr_ÇûQling_and_H£aLLng^ 1976, pp. 847.

15. Huang, B. J., and Chang, T. Y., "Design Analysis of Ammonia-Water Asorption Refrigeration System", 1078 Society of Automotive Engineers, Inc. Pro Intersic Energy Convers Eng Conf 13th, San Diego, Calif, Aug., pp. 20-25, 1978.

16. Wilur, Paul J., and Mitchell, Charles E., "Solar Asorption Air Conditioning Alteratives, 1975, Vol. 17, PP. 193-199.

17. Peng, C. S. P., and Howell, J. R., " Analysis and Design of Hyrid Doule-Asorption Cooling Systems for Low Grade Thermal Energy Application", Journal_of_Solar Energy Engineering - Nov. 1981, Vol. 103/331 .

18. Mansoori, G. ALi, and Patel, Vinod, "Thermodynamic Basis for the Choice of working Fluids for solar Asorption Cooling System", Solar_Energy. 1 979, Vol. 22, pp. 483-491.

19. Dubinin, M. M., and Astakhov, V. A., "Description of Adsorption Equilibriaot Vapors on Zeolites over Wide Ranges of Temperature and Pressure", MüLs.ç.ül·ar.-àiè.y.S. Zeolites - II, American Chemical Society,1971.

20. Guilleminot, J. J. "Application an Intermittent Cycle to Refrigeration" J^_J^_GlliIL£Ulino£_lhe.sis_Diipiu 1 97 8.

21. Dubinin, M. M., Kadlec, 0., and Zukal, A. "Adsorption Equilibria of Water on NaX Zeolite" M£1acи1ax_51ey.e Zeolites - II, American Chemical Society,1971.

22. Jones, J. B., and Hawkins, G. A. Engineering,Thermodynamics^_New York, Wiley, I 960.

23. Tennessee Valley Auttority. Çl·imaLlÇ-Dsta.Èaa^ Architectural Design Branch,1980.

VITA

Shih-Chieh Chang was born in Taiwan, Republic of China on Jan. 1, 1948. He received a diploma in Mechanical Engineering from Ming-Chi Institute of Technology which he attended from September, 1964 to June, 1969.

After graduating he worked as a full time teaching assistant in Ming-Chi Institute of Technology. He entered the University of Mississippi at Oxford in January, 1983. He expects to complete his master program in August, 1984.

In October of 1974, he was married to Bao-Lan Lay of Taiwan, Repulic of China.

S. C. Chang
Associate Professor of
Mechanical Engineering,
Ming-Chi Institute of Technology,
Taipei, Taiwan

J. A. Roux
Associate Professor of
Mechanical Engineering,
University of Mississippi,
University, Miss. 38677
Mem. ASME

Thermodynamic Analysis of a Solar Zeolite Refrigeration System

A solar zeolite-water absorption refrigeration unit was studied. Thermodynamic expressions were derived to predict the system performance. The operating range and optimum design parameters for the zeolite system were determined. The main parameters governing performance were: solar collector type, ambient temperature, and absorber properties. Results are shown for various solar collector types and various zeolite types. A desorption initiation temperature is shown to exist. The analysis is not based on empirical heat of absorption data, but rather on a zeolite properties relationship {log P_v versus 1 /T_z) to determine system performance.

Introduction

Much research has been performed on absorption refrigeration. These works can be classified into two types: intermittent, references [1-4], and continuous, references [5-10]. For the continuous solar absorption cooling cycle, several working fluids have been studied, references [5, 7, 9, 10]. Mansoori and Patel [11] have recommended NH_3-water, NH_3-NaSCN, and LiBr-water combinations as favorable candidates. The most serious disadvantage of the continuous absorption cycle is that heat cannot easily be rejected by an air cooler on hot days. However, the simple intermittent solar refrigeration can reject heat over a wide temperature range and only needs a simple and economic air cooler. The intermittent system can use either a liquid or a solid absorber. The total daily mass absorbed and desorbed in the intermittent system is usually a small percentage of the absorber mass. The absorption isotherms for zeolites have a very weak pressure dependence. This weak dependence of mass absorption on pressure yields the ability of absorbing significant quantities of refrigerant.

Dubinin and Astakhov [12] have studied and discussed the limiting mass absorption values for some zeolite-refrigerant pairs. The daily water mass absorption for a simple solar-powered unit is about 5 to 10 weight percent of the zeolite. Tchernev [2] has pointed out that for most refrigerant gases the maximum amount absorbed by a zeolite is about the same - 30 weight percent.

Guilleminot [13] was the first researcher to present a mathematical thermodynamic model for zeolite refrigeration. He used a complex empirical correlation and experimental data to calculate the zeolite heat absorption value and system *COP*. Tchernev [2] experimentally determined the overall *CP* for a solar zeolite refrigerator. Meunier and Mischler [3], treating the latent heat of evaporation as a constant, have determined the refrigerant desorption initiation temperature. They presented a comparison among three pairs (LiBr-water, zeolite (13X)-water, and zeolite (4A)-water). They found that the zeolite (13X) was always better than the zeolite (4A). Among the three pairs, the LiBr-water pair yielded the best performance for a heat sink temperature of 35°*C*. But, in the LiBr-water case, there was the difficult problem of crystallization at a heat sink temperature of 45°C. Thus the zeolite (13X)-water pair was best for the 50°C heat sink temperature. However, the initiation desorption temperature (temperature at which desorption begins) they computed was not realistic. The initiation desorption temperatures for different absorption pairs is not the same even under the same operating condition. The initiation desorption temperatures of reference [3] for these three pairs were given as the same temperature. Therefore the system overall *CP* presented in [3] must be corrected to account for the different initiation desorption temperatures.

The temperatures at which mass is desorbed is important because the desorption temperature range strongly affects the solar-collector efficiency. Here a zeolite properties equation related to its heat absorption value and the initiation desorption temperature has been derived. Using this expression it is shown how the system *CP* and heat absorption value are affected by the slope of the zeolite constant (water) mass line, the evaporation and condensation working temperatures, the ambient temperature, and the solar collector type.

Thermodynamic Analysis

The relationship [14] for the system overall *CP* can be expressed as

$$CP=\{COP_r\}\{_{Vp}\}\{_{Vco}\} \quad (1)$$

where *CP* is the ratio of the cooling effect to the total incident solar energy, η_{fv} is the solar collector efficiency, η_ρ is the power cycle efficiency, and COP_r is the coefficient of performance for the refrigeration cycle. These ideal Carnot cycle efficiencies are given by

$$\eta_\rho = \{T_H - T_L)/T_H; \quad COP_r = TJ\{T_H\text{-}T_L) \quad \text{(la)}$$

where T_H of the Carnot power cycle is the generator temperature *{Tf)* and T_L the ambient temperature $\{T_a\}$. The values T_H and T_L of the reverse Carnot cycle are the ambient

Contributed by the Solar Energy Division for publication in the JOURNAL OF SOLAR ENERGY ENGINEERING. Manuscript received by the Solar Energy Division, January, 1985.

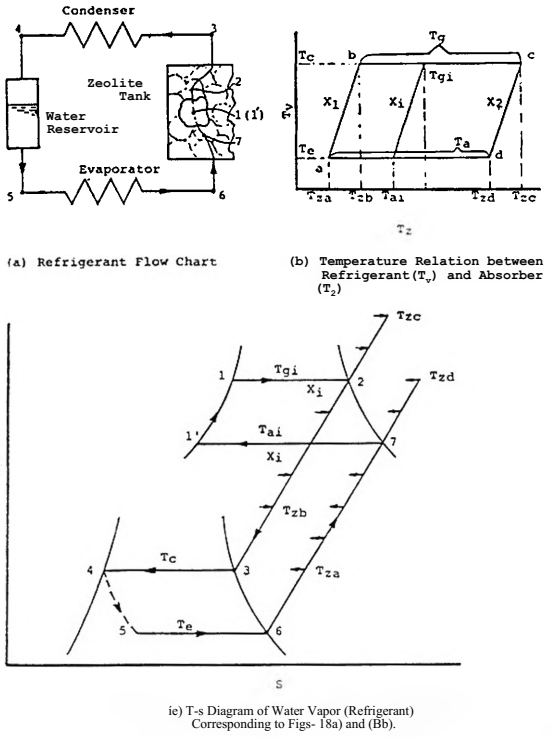

Fig. 1 Relationship between absorption properties and absorption refrigeration cycle

temperature, $T_{œ}$, and the evaporator temperature, T_e, respectively. Combining these terms yields the system overall *CP* from equation (1) as

$$CP_c = \left(\frac{T_g - T_\infty}{T_g}\right)\left(\frac{T_e}{T_\infty - T_e}\right)\eta_{co} \qquad (2)$$

Equation (2) can be applied to all kinds of solar vapor-compression refrigeration systems. For the absorption refrigeration system, the working temperature range in equation (2) must correspond to the absorption cycle. The vapor properties at each specific point in the cycle is illustrated by a *T-s* diagram as in Fig. 1. Figure 1(a) shows the flow chart of the absorption refrigeration system. The refrigerant (water vapor) temperature versus absorber temperature is shown in Fig. 1(6). The *T-s* diagram related to this system is shown in Fig. 1(c). It should be noticed that the absorption and desorption processes occur at different temperatures T_{ai} and T_{gi} (which are determined according to their instantaneous mass concentration, X_i, as shown in Fig. 1(6). However, the absorption and desorption processes can be classified as many pairs that have a fixed sorbent mass concentration. Assuming the temperature of the zeolite is uniform, then at any instant the zeolite will be at some mass sorbent concentration, $X_{,}$ at which a given evaporation and condensation pressure yields two corresponding absorption and desorption temperatures T_{ai} and T_{gi} (Fig. 1(6)). The desorption and absorption processes under this instantaneous mass concentation are indicated by lines 1-2 and 7-1 ' (Fig. 1(c)), respectively. It can be seen that the refrigeration cycle is marked by 3-4-5-6, while the power cycle is marked by 7-Γ -1-2. The maximum system *CP* (Carnot cycle) has been presented in equation (2).

For the absorption cycle the working temperature range in the power cycle is limited by the absorption and desorption temperature range (as indicated by T_a and T_g in Fig. 1(6)). Due to the relationship between the instantaneous absorption and desorption temperatures, the desorption temperature

---------- Nomenclature ----------

a = end point of absorption process in absorption cycle
6 = starting point of desorption process in absorption cycle
c = end point of desorption process in absorption cycle
$C_{a>}$ = constant for the solar collector efficiency equation, equation (26)
C_L = constant for the heat of evaporation equation (kj/kg), equation (17)
C- = constant for the zeolite-water property equation, equation (20)
C_{pz} = specific heat of zeolite (kj/kg K)
CP = instantaneous ratio of cooling effect to incident solar energy
CP_c = CP for Carnot cycle limited by ambient and heat source temperatures
$CP^{\wedge}$ = CP for Carnot cycle according to absorption refrigeration temperatures
CP_a = CP based on absorption refrigeration cycle
CP_m, = mean CP defined in equation (29)
$CP_{,,}$ = mean CP defined in equation (30)
COP = ratio of cooling effect to heat consumption of generator
COP_r = ratioof cooling effect to work input
COP_c = system COP based on Carnot cycle
COP_U = system COP based on absorption refrigeration cycle
d = starting point of absorption process in absorption cycle
h = enthalpy of water vapor (kj/kg)
ΔH = heat of absorption (kj/kg)
L = latent heat of vaporization (kj/kg)
m_{co} = solar collector efficiency slope, equation (26)
m_L = slope of heat of evaporation line, equation (17)
m_z = slope of a constant mass line on log P_v versus l/Tį plot, equation (20)
M = mass (kg)
P = pressure (bar)
Q = heat(kj)
R = water vapor gas constant (kj/kg K)
S = entropy (kj/kg)
T = temperature
T_H = high-working temperature in Carnot cycle (K)
T_L = low-working temperature in Carnot cycle (K)
T_a = absorption temperature (K)
T_g = desorption temperature at generator (K)
T_{za} = temperature at which absorption process end; (K)
T_{zb} = temperature at beginning of desorption (K)
$T_{4'}$ = temperature at which desorption process end: (K)
T_{zd} = temperature at beginning of absorption (K)
X = weight ratio of absorbed water to solid zeolite
a = absorption
ab = absorber
c = condenser
C = Carnot
co = collector
e = evaporator
f = liquid state, final state
f = counter index
v = vapor
w = water
z = zeolite
oo = ambient

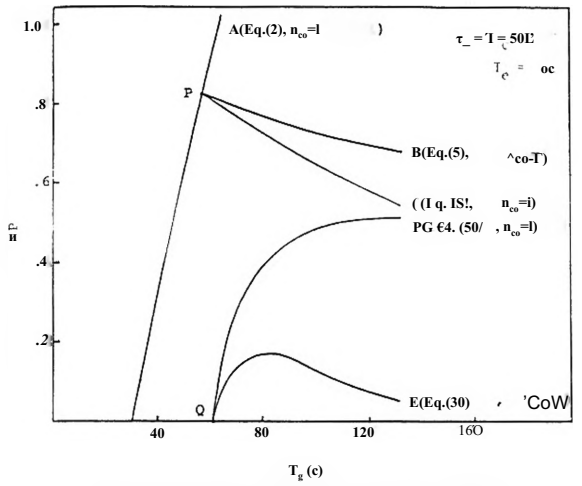

Fig. 2 System CP versus generator temperature

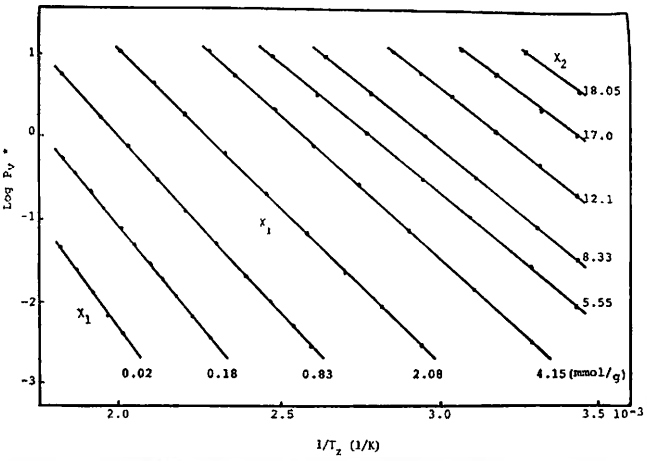

Fig. 3 The log versus UT_n plot for zeolite NaX-water pair from experimental data 115]; "P_v (mmHg)

must increase as the absorber temperature increases. Hence the working temperature T_L (= T_a) of the power cycle must also increase. Therefore the instantaneous Carnot cycle *CP* for the absorption working temperature can be written as

$$CP_{ca} = \left(\frac{T_g - T_a}{T_g}\right)\left(\frac{T_e}{T_\infty - T_e}\right)\eta_{co} \qquad (3)$$

Equation (3) is based on the Carnot cycle, but the working temperature range is limited by the absorption temperature range(7^ and T_{ai} in Fig. 1(b)).

To consider the phase transformations involved in the absorption-desorption processes of the foregoing case, a more realistic limitation for the system *CP* can be derived by employing the Clausius-Clapreyon relation for the phase transformations. For an absorption system, the theoretical overall *CP* can also be expressed as follows

$$CP_a = (COP_r)(V_{pa})(V_{co}) \qquad (4)$$

By the definition of COP_r and $\eta_{\rho\alpha}$ this can be written as

$$CP\,a = \left(\frac{\text{Work Out}}{Q_{in}}\right)\left(\frac{\text{Cooling Load}}{\text{Work In}}\right)\eta_{co} \qquad (\$)$$

Since the work output of the absorption power cycle must be equal to the work input to the refrigeration cycle, equation (5) reduces to

$$\eta_{CPa} = \frac{\text{Cooling Load}}{Q_{in}}\,\eta_{co} \qquad (5)$$

The cooling load will be equal to the latent heat of vaporation, *L,* in the evaporator. The heat input, Q_{in} is equal to the heat absorption value, Δ77, in the absorption process. Thus the overall absorption system efficiency, considering the phase transformation in the absorption process, becomes

$$\eta_{Pa} = \eta_{co}\,LATI \qquad (6)$$

As seen in Fig. *1(b),* the heat absorption process occurs between the evaporator pressure *(P_e)* and the condenser pressure *(P_c).* The heat absorption value *AH* can be determined from the Clausius-Clapreyon equation for an equilibrium phase transformation. Applying the Clausius-Clapreyon relation to the vapor-liquid transformation in the zeolite yields

$$d(\ln P)/dT = AH/RT^2 \qquad (6a)$$

Integration of equation (6a) between $P_e(T_a)$ and $P_c(T_g)$ of Fig. 1(b) yields

$$In\,(Pc/Pe) = \int_{T_\alpha}^{T_g} (AH/RT)dT \qquad (6b)$$

For the liquid-vapor transformation in the evaporator the Clausius-Clapreyon relation can be written as

$$d(\ln P)/dT = L/RT^2 \qquad Va)$$

Integration of equation (7a) between P_e (T_e) and P_c (T_c) of Fig. 1(b) yields

$$\ln(P_c/P_e) = \int_{T_c}^{T_c} (L/RT^2)dT \qquad (7b)$$

Combining equations (6), *(6b),* and *(7b)* and taking *L* and *AH* as constants yields

$$CT = \left(\frac{T_c - T_e}{T_c}\right)\eta_{co} \qquad (8)$$

where equation (8) is for an infinitesimal shift of composition.

Figure 4 shows that equation (8) is very close to equation (3) and both equations intersect at point *P* (where $T_{ai} = T_x$; T_{ai} and T_{gj} are the absorption and desorption temperatures for mass, concentration X_i). Equation (8) provides an instantaneous overall system *CP* for the absorption cycle. This is the limitation of system performance valid for all solar absorption refrigeration systems.

Absorber Properties Equation. To derive a simple absorber properties equation for the absorption process it was assumed that the constant mass concentration line was linear in the coordinates of log P_v versus $1/T_{ab}$. It was shown by Dubinin and Serpinsk [15] that the linearity of the constant (water) mass lines (Fig. 3) is in agreement with the theory of volume filling of microporous absorbents (zeolite). Under the linearity assumption, the absorber properties relation can be expressed as

$$\log P_v = -m\left(\frac{1}{Tg}\right) + C \qquad (9)$$

Equation (9) is a general form of the absorber properties relation. To apply equation (9) for computing T_a and T_g it is necessary to differentiate equation (9) and write it in the following form

$$m = \frac{-d\log Pv}{d(1/Tg)} \qquad (10)$$

Now equation (6a) can be written as

$$\Delta H = RT^2\left(\frac{d\log P}{dT}\right) \qquad (\Pi)$$

Combining equations (10) and (11) and simplifying gives the expression for *AH* as

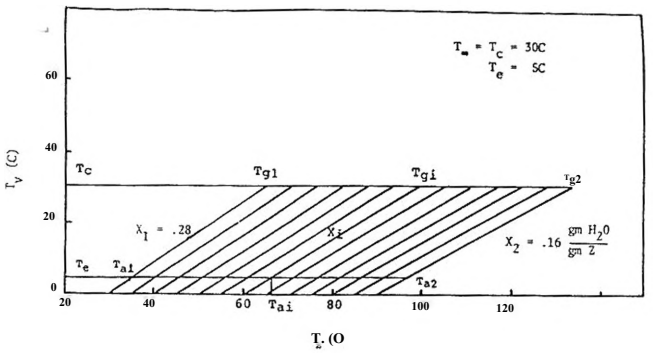

Fig. 4 *Ty* versus T_z plot for zeolite (13X)-waterpair

$$\Delta H = Rme\left(e = \frac{ln\ P}{\log P}\right) \tag{12}$$

This expression shows that the heat absorption value, Δ77, is only a function of the slope, *m,* of the constant mass line on a log P_v versus l/T_{ab} plot. All the points along a given constant mass line have the same slope (Fig. 3). Therefore each point along the same constant mass concentration line has the same heat absorption value, *AH.*

To change the coordinates from P_v versus $\backslash/T_{ab}$ to T_v versus $\backslash/T_{ab}$, it is necessary to know the relationship between P_v and T_v. To determine this relationship the Claperyon equation was employed between the phase equilibrium state of the liquid and the vapor; therefore from [16] the Claperyon equation can be written as

$$\frac{dP_v}{TI\backslash \sim TA^{\wedge}\text{-}Vf)} \tag{13}$$

Using the ideal gas equation of state for the vapor and realizing that $Vj << v_v$, equation (13) becomes

$$\frac{d\,P_v}{P_v} = L\left(\frac{d\,T_v}{R\,T_v^{\,2}}\right) \tag{14}$$

Now from equations (6a) and (12) for the absorber and using the ideal gas equation of state and simplifying yields

$$ùH = Rme = RT^{\wedge}(-^{\wedge}r\}(dP_v) \text{—} E\text{-} \frac{\backslash RT_V/}{d\,T_{ab}} \tag{15}$$

Combining equations (14) and (15) gives the result

$$Rme = \left(\frac{T_{ab}^{\,2}}{T_v^{\,2}}\right)\left(\frac{Ld\,T_v}{d\,T_{ab}}\right) \tag{16}$$

In reality the value *L* for water is a very weak function of temperature. For the zeolite-water pair this functional dependence can be written for water as

$$L^{\wedge}m_b T_v + C_L \tag{17}$$

Inserting equation (17) into equation (14) yields

$$\frac{d\,P_v}{P_v} = \frac{d\,T_v}{(m_L\,T_v + C_L)\,R\,T_v^{\,2}} \tag{18}$$

Integration of equation (18) gives the P_v versus T_v relationship for the water vapor (absórbate) in the phase transformation as

$$in\ P_{L\cdot} = -\left(\frac{C_L}{R}\right)\left(\frac{1}{T_v}\right) + m_L(\backslash/R)ln\ T_v + C_w \tag{19}$$

where C,, is a constant (C_w = 48.11 bar) when *T,* varies from 0 to 30°C. For the zeolite-water pair, equation (19) can be written as

$$In\ P_v = em.\ \text{-}\left(C_{\text{-}}\frac{-1}{T_z}\right) \tag{20}$$

where C_z is a constant for each different constant mass line (see Fig. 3). Now combining equations (19) and (20) gives

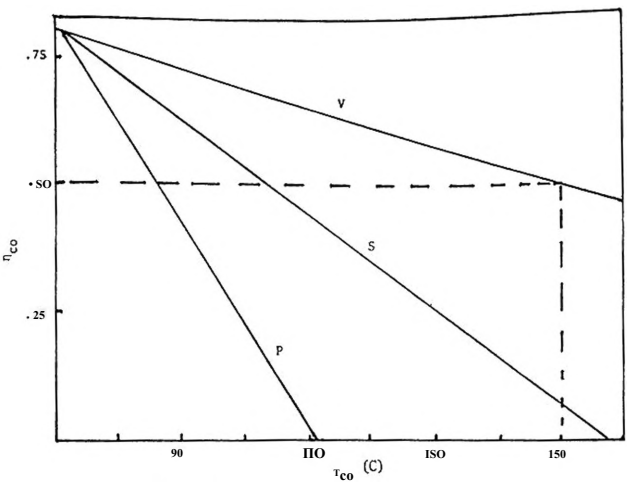

Fig. 5 Solar collector performance

$$\frac{em_z}{\text{^}T_{\text{»}}} + eC_z = C_w\text{-}(^{\wedge}\text{-}\backslash/T_v\} \quad + m_L(l/R)ln\ T \tag{21}$$

This relationship, equation (21), is based on the zeolite-water pair phase transformation. Using this expression one can plot the isoster of T_v versus T_z for *L* being a function of temperature (shown in Fig. 4). Now equation (21) can be written to explicitly determine *T.* as

$$T_z = \frac{-m.e}{C_w\text{--}^{\wedge}+\frac{C}{KI}m_L(\backslash/R)ln \quad T_v\text{—}eC_z} \tag{22}$$

Equation (22) shows the relationship between absorber and absórbate temperatures. Where C_z is a constant on the same constant mass line. Taking data of T_z, P_v, and m_z from any point (on an żth constant mass line), C_z of the ′th constant mass line can be computed as

$$C_{,} = \frac{I\,/\,C_L}{e^{\text{-}}}\ (c_w\text{-}^{\wedge}+m_L(l/R)ln \quad T_v \quad + \frac{em\ \backslash}{T_{z\cdot}}\text{-J} \tag{23}$$

where $T_z = T_{zi}$. Inserting C_{zh} equation (23) into equation (22), the żth constant mass line in T_v versus $T_{\cdot}$ coordinates can be obtained. The T_c versus $T_{\cdot}$ line for each żth constant mass line is nearly a straight line (Fig. 4). The temperature of desorption for each line is the location where the vapor condensation temperature (T_v) equals T_c. Thus the desorption temperature for the zth constant mass line can be expressed as

$$T_{\ S>\ C} = \frac{\text{—}\ em_{zi}}{C_{\text{--}}\text{-±-+}rn_L min\ T_c\text{-}C_{zi}e} \tag{24}$$

Also the absorption temperature for each zth line is the location where the corresponding evaporator vapor temperature is T_e. Therefore the absorption temperature can be expressed as

$$T_{o\cdot} = \frac{-em.,}{C_K\text{-}\frac{C_I}{RT_c} \quad + m,(1/R)In\ T_c\text{ - }eC.,} \tag{25}$$

Equations (24) and (25) show the refrigerant (absórbate) desorption and absorption temperatures are both related to the absorption pair properties.

Relationship Between Solar Collector Efficiency and Absorption Properties. There are several types of solar

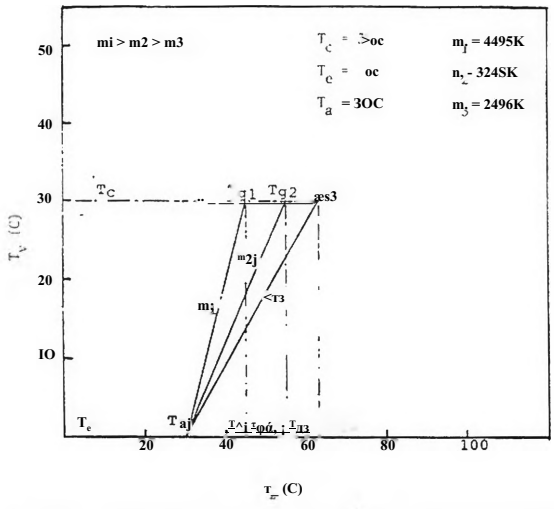

Fíg. 6 Effect of the slope, *m,* on desorption temperature based on equation (24)

collectors. The three types considered here for flat-plate solar collectors are (1) S-type (single-glazing), (2) P-type (double-glazing), and (3) V-type (evacuated). The collector efficiencies of these three types are nearly a linear function of collector temperature, as shown in Fig. 5. A mathematical expression for the efficiencies of these three types of collectors can be expressed as

$$Vco = {}^{m}\,co\,T_{l0} + {}^{C}co \qquad (26)$$

where m_{co} and C_{co} are constants and depend on the type of solar collector. More complicated expressions relating collector efficiency and collector temperature could be used in place of equation (26). For simplicity, the temperatures of the collector and zeolite were assumed to be equal. This implies the heat exchanger (coupling heat transfer between the zeolite and the solar collector) efficiency is equal to unity. Until the zeolite reaches the initiation desorption temperature, there is no mass circulating in the refrigeration cycle, thus the *CP* will be zero. After reaching the initiation desorption temperature, there is some mass circulating in the refrigeration cycle and the system *CP* will increase gradually. The temperature of the zeolite will be equal to the desorption temperature of each /th constant mass line. This means that T_{co} (collector temperature) = T_z, = T_g after the beginning of desorption. Employing equation (24) *{*T_{co} = T_{gl}*)* and combining with equation (26) yields

$$\eta_{co} = m_{co}\left(\frac{-em_{zi}}{C_w - \dfrac{C_L}{RT_c} + m_L\dfrac{\ln T_c}{R} - eC_{zi}}\right) + C_{co} \qquad (27)$$

Equation (27) shows that the solar collector efficiency is also affected by the absorption properties (constants m_v and *C^),* and the solar collector type (constant m_{co} and C_{co}*).*

Instantaneous *CP* for Solar Zeolite Refrigeration System. Combining equations (27), (6), and (15) gives the result

$$CP_{ul} = \frac{-L}{eRm.j}\left(\frac{-e(m.j)\,(m_{co})}{C' - \dfrac{C_L - m_L(\ln T_c)}{RT_c R} - eC_{zi}} + C_{co}\right) \qquad (28)$$

Equation (28) shows the instantaneous system *CP* is affected

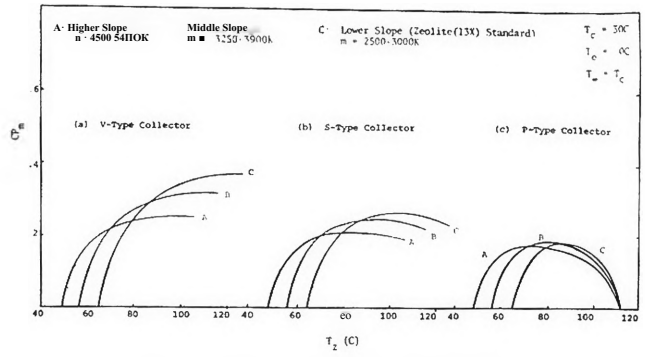

Fig. 7 Effect of nonuniform zeolite slope

by: (1) absorber properties *(*m_{zi} and C.,), (2) working temperatures T_c and T_e, in the refrigeration cycle, and (3) solar collector types *(*m_{co} and C_{co}*).* Recall that the zeolite properties equation constants, C_{ZI}, are related to T_{ZI}, where T_{zi} are dictated by the ambient temperatures. Thus the instantaneous system *CP* is also determined by the ambient (condenser) temperatures.

Mean *CP* for Zeolite Refrigeration System. The instantaneous system *CP,* equation (28), has been derived by considering the working fluid properties (per Ibm basis), but the amount of working fluid has been ignored. For the absorption system the working fluid comes from mass desorbed at the absorber. Instantaneous system *CP* is not meaningful without quantifying the working fluid mass. The mean system *CP* of the zeolite absorption system is defined as

$$CP_{mt} = \frac{\sum_{i=1}^{2}[L(X_i - X_{i-1})]}{\sum_{i=1}^{2}\left[(X_i - X_{i-1})\dfrac{(\text{ДЯ}^{\wedge}+\text{АЯ},)}{2\eta_{O/}}\right]} \qquad (29)$$

where X_j is the water mass concentration at the beginning of the entire desorption process. The value X_2 is the concentration at the end of the entire desorption process. The symbol *X,* is the concentration at the /th constant mass line between X_x and X_2. Accounting for the sensible heats (thermal capacity) of the generator (sorbent and sorbate) will reduce the performance given by equation (29). Allowing for the influence of these thermal capacities yields

$$CP_{,,} = \frac{\Sigma^{\wedge}X\text{-}x.\text{-}^{\wedge}\text{-}Qy}{\sum_{/=1}^{2}\left[\text{A},\text{—}X_{\_}^{\_}\,!\right)\dfrac{(\Delta H_{i-1}+\Delta H_i)}{^{\wedge}coj^{J}}\right] + \text{У?}^{-} + \text{Уз}^{-}} \qquad (30)$$

where *Q\,* the heat necessary to cool the sorbate from T_c to T_e is given by

$$Q^{\wedge}\Sigma^{\wedge}\chi_{I}\text{-}\chi i\text{-}^{\wedge h}c\text{-}h_e)] \qquad (31)$$

Q2, the heat necessary to bring the mass of the sorbate (1) from T_{za} to T_{zh} (X_a constant) and (2) from T_{zh} to T_{zc} (*X,* not constant), is given by

$$a = \sum_{i=a}^{g2}\left[*\pm i\,11 + \text{V}_{L}\,\Gamma\,\frac{X_i(h_i - h_{i-1})}{Vco,}\right] \qquad (32)$$

Q3, the heat necessary to bring the mass of the sorbent from T_{za} to T_{zc} ($m_{.}$ constant), is given by

$$Q, = \sum_{i=1}^{n} Cp.(Ta-Tu-)\frac{11}{\text{coi}} \qquad (33)$$

Results

The dependence of the system *CP* as a function of generator temperature is shown by the five curves *(A, B, C, D,* and *E)* in Fig. 2, where curves *C, D,* and *E* correspond to zeolite 13-X. Curve *A* represents the Carnot cycle efficiency (equation (2)); curve *B* represents the Carnot cycle efficiency based on the absorption working temperature (equation (3)). Curve *C* represents the absorption cycle efficiency (equation (8)); curve *D* represents the mean absorption cycle efficiency (equation (30)), assuming a solar collector efficiency of unity. Curve *E* represents the mean absorption cycle efficiency (equation (30)) based on a solar collector efficiency which is a function of temperature. Before reaching the initiation desorption temperature there is no working fluid mass in the refrigeration cycle. Since there is no mass flow, curves *D* and £ in Fig. 2 are zero until reaching point $Q\{T_a = T^{\wedge})$, which is the initiation desorption point. Points *P* and *Q* are the same initiation desorption temperature. The mean CP_m (curve *D)* increases sharply when T_K increases beyond point *Q,* however as T_g increases the instantaneous *CP* (curve *B)* eventually begins to decrease; this causes the mean value (curve *D)* to decrease. Therefore a maximum mean CP is achieved after *7^* increases beyond point *Q* on curve *D.* Since the solar collector efficiency also decreases as T_K increases, the system overall mean $CP_{,,}$ (curve *E)* will decrease more sharply than curve *D.*

Since high temperatures yield low solar collector efficiencies, a low desorption temperature is related to the absorption properties as shown in equation (24). These absorption properties depend on the absorption pair and can be represented by the constant mass lines on a log P_v versus $\backslash/T_z$ plot. One of the main parameters for the constant mass lines is the slope, m_z. To see how the refrigerant desorption initiation temperature will be affected by a different absorption pair, equation (24) has been employed by holding all parameters constant except the slope, m_z. The results are shown in Fig. 6; here higher m_z values result in lower desorption temperatures. Therefore the desorption initiation temperature for three different absorption pairs which start at the same point, T_o (as represented by reference [3]) does not agree with equation (24). To show this effect the set of slopes for the zeolite (13X)-water pair (reference [13]) was chosen. Then by varying each constant mass line slope by a constant factor, a simulation of various types of zeolite-water pairs was achieved. To show how the system $CP_{,,}$ was affected by the nonuniform slopes of the zeolite mass absorption properties, equation (30) was used to compute the $CP_{,n}$ values. The results are shown in Fig. 7 where the solar collector performances are shown in Fig. 5. In Fig. 7 there are three curves, *A, B,* and *C.* They are generated by taking X_z = 0.280-0.190, and C_{pz} = 0.963 (kj/kg K). Curve *C* (m_z = 2500-3000) is the standard zeolite (13X)-water pair and represents the lower-slope type of zeolite-water pairs. Curve *B* [m_z = 3250-3900) represents the results of the middle-slope type of zeolite-water pairs, and curve *A* (m_z = 4500-5400) represents the high-slope type. Curves *A, B,* and *C* in Fig. 7 each have a different initiation desorption temperature. The lower-slope type always has the highest initiation desorption temperature. Also the maximum $CP_{,n}$ is quite different for curves *A, B, C,* (Fig. 7) which corresponds to the V-type solar collector. The maximum $CP_{,,}$ values for the P-type solar collector are essentially equal.

The starting points on curves *A, B, C* (in Fig. 7) are the initiation desorption points. These separate initiation desorption points shown on curves *A, B, C* can be deduced from equation (24) and agree with the trend of Fig. 6. A low initiation desorption temperature allows the solar collector to operate at a lower temperature range but has a higher slope (m_z) value which implies having a higher heat absorption value (see equation (12)). Therefore the slope, m_z, has competing effects. (1) The higher slope helps the system CP_m by operating at lower generator temperatures and hence higher solar collector efficiencies. (2) The higher slope has higher heat absorption values which lowers the refrigeration cycle COP_r value (see equation (6)). Hence there are two coupled effects governing the system overall CP_m as a function of the slope, m_z. Due to these two combined effects the results in Fig. 7 become clear. (1) For a system using an evacuated solar collector, the collector efficiency is a weak function of temperature and hence is not strongly affected by the desorption initiation temperature. Therefore CP_n, is primarily influenced by the second effect (a low heat of absorption value) which causes a higher overall CP_m to be achieved by the lower m_z (curve *C).* (2) For the system using a P-type solar collector, the collector efficiency will drop sharply as the working temperature increases, thus both the effects of varying the slope, m_z, are competing in such a manner that Fig. 7(c) indicates only a weak influence on the maximum CP_m for the three different curves *A, B,* and *C.* In summary, the heat of absorption value is not important to the zeolite absorption refrigeration system maximum performance if a simple P-type flat-plate solar collector was used.

Conclusions

The system performance was found to depend primarily on the solar-collector type and the zeolite absorption properties. These absorption properties depend on the absorption pair and can be represented by the constant mass lines on a log P_v versus i/T_z plot. The slope, m_z, was found to be the only variable for determining the heat absorption value, *AH.* A line of constant mass concentration will also be a line of constant heat absorption valve. The slope, m_z, has competing effects on the system performance. (1) The higher slope (lower desorption temperature) helps the system performance by operating at lower generator temperatures and hence higher solar collector efficiencies. (2) The higher slope (higher *AH* value) lowers the refrigeration cycle COP_r and hence lowers the overall efficiency. Therefore a higher CP_m will be achieved by a lower m_z value when using a V-type collector and by a higher m_z value when using a P-type collector.

The instantaneous solar *CP* is affected by: *(a)* the absorber properties (m_{zi} and c_{zi}), *(b)* the working temperature T_c and T_e in the refrigeration cycle, (c) the solar collector type, and *(d)* the ambient temperature. In the summer time (ambient temperature assumed 30°C), the CP_m at 100°C will be around 0.12-15 for the P-type solar collector, it will be 0.19-0.24 when using a S-type solar collector at T_g = 100°C, and can reach a value of about 0.4 for the V-type solar collector when T_g is 120°C.

References

1 Venkatesh, A.,; Sriramulu, V., and Gupta, M. C., "Theoretical and Experimental Investigation of an Intermittent Solar Refrigerator,'' *Sun II,* Vol. 1, 1979, pp. 749-753.

2 Tchernev, D. 1., "Solar Energy Application of Natural Zeolites," *Natural Zeolite and Its Use,* Oxford, New York, Pergamon Press, 1978, pp. 479-484.

3 Meunier, F., and Mischler, B., "Solar Cooling Through Cycles Using Microporous Solid Adsorbents," *SUN II,* Vol. 1, 1979, pp. 676-680.

4 Meunier, F., Mischler, B., Guilleminot, J. J., and Simonot, "On the Use

of a Zeolite 13X-H_2O Intermittent Cycle for Application to Solar Climatization of Buildings," *SUNII,* Vol. 1, 1979, pp. 739-743.

5 Alizadeh, S., Bahar, F., and Geoola, F., "Design and Optimization of an Absorption Refrigeration System Operated by Solar Energy," *Solar Energy,* Vol. 22, 1979, pp. 149-154.

6 Stoecker, W. F., and Reed, L. D., "Effect of Operating Temperatures on the Coefficient of Performance of Aqua-Ammonia Refrigeration Systems," Part 1, *ASHRAE Trans.,* 1971, pp. 163-170.

7 Bessler, W. F., and Chen, C. N., "Study on Parameter Variations for Solar Powered Lithium Bromide Absorption Cooling," *Solar Cooling and Healing,* 1976, p. 847.

8 Huang, B. J., and Chang, T. Y., "Design Analysis of Ammonia-Water Absorption Refrigeration System," *1978 Society of Automotive Engineers, Inc. Pro Intersic Energy Convers Eng. Conf. 13th,* San Diego, Calif., 1978, pp. 20-25.

9 Wilur, P. J., and Mitchell, C. E., "Solar Absorption Air Conditioning Alternatives," *Solar Energy,* Vol. 17, 1975, pp. 193-199.

10 Peng, C. S. P., and Howell, J. R., "Analysis and Design of Hybrid Double-Absorption Cooling Systems for Low Grade Thermal Energy Application, ASME JOURNAL OF SOLAR ENERGY ENGINEERING, Vol. 103, Nov. 1981, p. 331.

11 Mansoori, G. A., and Patel, V., "Thermodynamic Basis for the Choice of Working Fluids for Solar Absorption Cooling System," *Solar Enerev* Vol 77, 1979, pp. 483-491.

12 Dubinin, M. M., and Astakhov, V. A., "Description of Absorption Equilibriaot Vapors on Zeolites Over Wide Ranges of Temperature and Pressure," *Molecular Sieve Zeolites—II,* American Chemical Society, 1971.

13 Guilleminot, J. J., "Application of an Intermittent Cycle to Refrigeration," J. J. Guilleminot Thesis, University of Dijon, France, 1978.

14 Chang, S. C., "Solar Zeolite Refrigeration System," M.S. thesis, University of Mississippi, Aug. 1984.

15 Dubinin, M. M., Kadlec, O., and Zukal, A., "Absorption Equilibria of Water on NaX Zeolite," *Molecular Sieve Zeolites—II,* American Chemical Society, 1971.

16 Jones, J. B., and Hawkins, G. A., *Engineering Thermodynamics,* Wiley, New York, 1960.